iScience

CellPress
OPEN ACCESS

Article

Post-transplant cyclophosphamide prevents xenogeneic graft-versus-host disease while depleting proliferating regulatory T cells

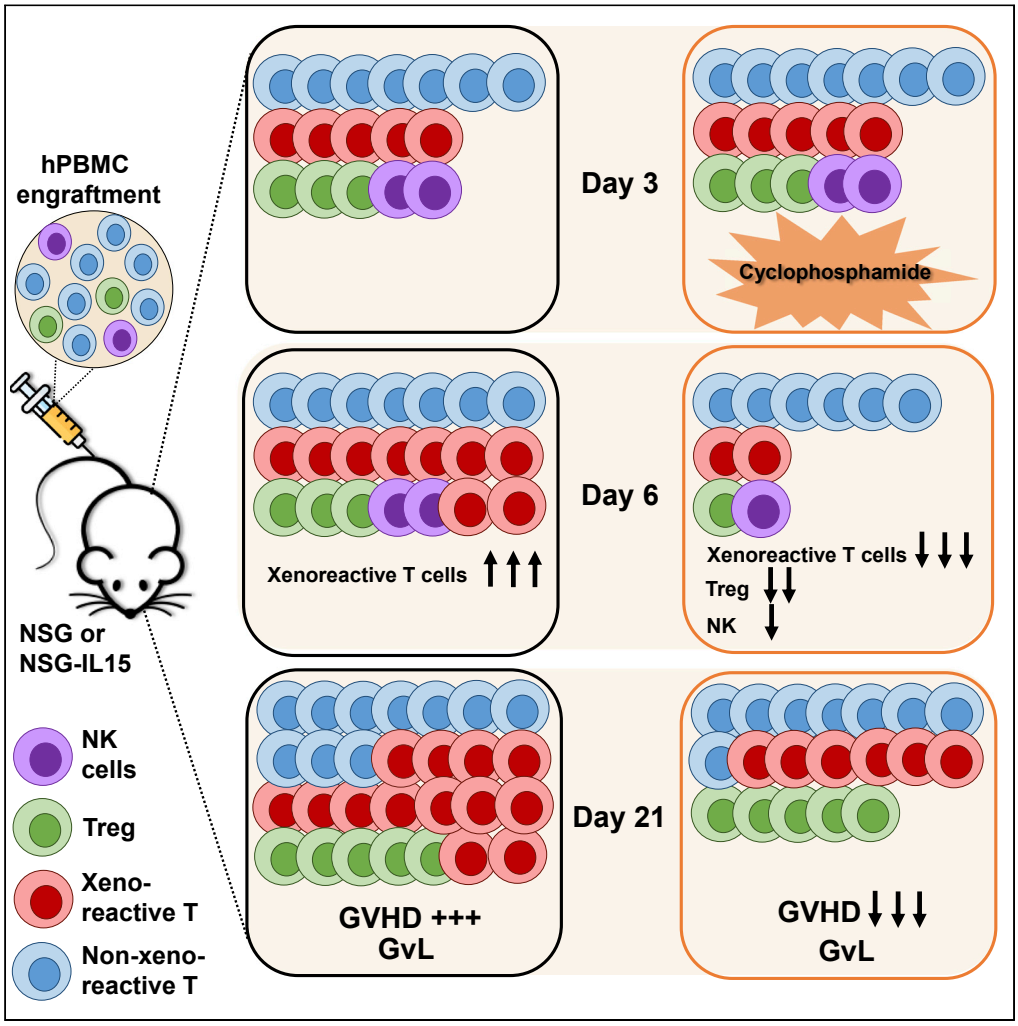

Caroline Ritacco, Murat Cem Köse, Justine Courtois, ..., Yves Beguin, Grégory Ehx, Frédéric Baron

g.ehx@uliege.be (G.E.)
f.baron@uliege.be (F.B.)

Highlights

Post-transplant cyclophosphamide prevents GVHD by depleting alloreactive T-cells

Post-transplant cyclophosphamide depletes proliferative regulatory T cells

Post-transplant cyclophosphamide does not abrogate graft-versus-leukemia effects

Ritacco et al., iScience 26, 106085
March 17, 2023
https://doi.org/10.1016/j.isci.2023.106085

iScience

CellPress
OPEN ACCESS

Article

Post-transplant cyclophosphamide prevents xenogeneic graft-versus-host disease while depleting proliferating regulatory T cells

Caroline Ritacco,[1] Murat Cem Köse,[1] Justine Courtois,[1] Lorenzo Canti,[1] Charline Beguin,[1] Sophie Dubois,[1] Benoît Vandenhove,[1] Sophie Servais,[1,2] Jo Caers,[1,2] Yves Beguin,[1,2] Grégory Ehx,[1,3,*] and Frédéric Baron[1,2,3,4,*]

SUMMARY

Graft-versus-host disease (GVHD) remains a serious limitation of allogeneic hematopoietic cell transplantation (allo-HCT). While post-transplant administration of cyclophosphamide (PTCy) is increasingly used as GVHD prophylaxis, its precise mechanisms of action and its impact on graft-versus-leukemia effects have remained debated. Here, we studied the mechanisms of xenogeneic GVHD (xGVHD) prevention by PTCy in different humanized mouse models. We observed that PTCy attenuated xGVHD. Using flow cytometry and single-cell RNA-sequencing, we demonstrated that PTCy depleted proliferative CD8$^+$ and conventional CD4$^+$ T cells but also proliferative regulatory T cells (Treg). Further, T-cell receptor β variable region sequencing (TCRVB) analyses demonstrated that highly xenoreactive T-cell clones were depleted by PTCy. Although Treg frequencies were significantly higher in PTCy-treated than in control mice on day 21, xGVHD attenuation by PTCy was not abrogated by Treg depletion. Finally, we observed that PTCy did not abrogate graft-versus-leukemia effects.

INTRODUCTION

Graft-versus-host-disease (GVHD) remains a serious limitation of allogeneic hematopoietic cell transplantation (allo-HCT).[1,2] However, GVHD occurrence has also been associated with graft-versus-leukemia (GvL) effects, the main mechanism of cure after allo-HCT.[3–5] While the association of a calcineurin inhibitor and an antimetabolite with or without anti-thymocyte globulins (ATG) has remained the standard GVHD prophylaxis in the last decades,[6,7] post-transplant administration of cyclophosphamide (PTCy) has proven to be an efficient way to prevent GVHD, not only in the HLA-haploidentical allo-HCT setting but also in HLA-matched or 1/10 HLA-mismatched allo-HCT.[8–12] However, the precise mechanisms of GVHD prevention by PTCy (and particularly the potential role of regulatory T cells (Treg)) remains debated.

Two seminal studies have investigated the anti-GVHD mechanisms of PTCy. First, using two mouse-to-mouse models of GVHD, Ganguly et al. demonstrated that effective GVHD prevention by PTCy required the presence of Treg which were found to be relatively resistant to PTCy.[13] Secondly, Kanakry et al. observed that PTCy decreased conventional T cells but favored Treg recovery in patients given PTCy-based GVHD prophylaxis. This was attributed to a protective expression of aldehyde dehydrogenase (ALDH) by Treg.[14] Accordingly, another recent study evidenced higher Treg counts but lower naive T-cell counts in patients given PTCy-based GVHD prophylaxis, as well as an overexpression of multiple inhibitory receptors on both CD4$^+$ and CD8$^+$ T cells in PTCy-treated patients.[15] In contrast, a recent large study observed comparable Treg recovery with PTCy and ATG-based GVHD prophylaxis.[16] Further, a recent nice systems biology analysis in patients given PTCy-based GVHD prophylaxis demonstrated that signatures of active and highly suppressive Treg were paradoxically enriched in patients experiencing acute GVHD.[17]

In the last decades, many advances have been made in our understanding of the pathogenesis of xenogeneic GVHD (xGVHD) induced by the injection of human peripheral blood mononuclear cells (hPBMC) in NOD.Cg-Prkdcs^{cid} Il2rgt^{m1Wjl}/SzJ (NSG) or in NOD/Shi-scid/IL-2Rγnul mice ("humanized" models of

[1]Hematology Research Unit, Groupe Interdisciplinaire de Génoprotéomique Appliquée (GIGA)-I[3], University of Liège, Liège 4000, Belgium

[2]Department of Medicine, Division of Hematology, CHU of Liège, Liège 4000, Belgium

[3]Senior author

[4]Lead contact

*Correspondence: g.ehx@uliege.be (G.E.), f.baron@uliege.be (F.B.)

https://doi.org/10.1016/j.isci.2023.106085

GVHD). It was found that xGVHD is caused by the activation of mouse MHC-reactive human T cells by murine hematopoietic antigen-presenting cells.[18,19] These activated T cells then upregulate the expression of genes involved in cell proliferation, T-cell receptor (TCR) signaling, co-stimulation, IL-2/STAT5, mTOR, and Aurora kinase A pathways (as observed in a non-human primate model of GVHD[20]). Activated T cells then acquire a T-helper 1 phenotype and migrate to xGVHD-target organs (mainly the bone marrow (BM), lungs, and liver), causing the disease.[21]

We recently investigated the mechanisms of GVHD prevention by the mTOR inhibitor rapamycin in humanized mouse models.[22] Looking at strategies that could potentiate the anti-GVHD mechanisms of rapamycin, we observed that PTCy mitigated xGVHD and thereby confirmed the initial observation by Kanakry et al.[14] Further, we observed higher frequencies of Treg in PTCy-treated mice on day 21 after hPBMC infusion. These initial observations prompted us to decipher herein the impact of PTCy on xGVHD and GvL effects with a special focus on Treg in humanized mouse models of GVHD.

RESULTS

Post-transplant administration of cyclophosphamide delays xenogeneic graft-versus-host disease

We first confirmed our prior observations that a single PTCy injection (100 mg/kg on day 3) prevented xGVHD induced by injecting hPBMC in NSG mice (n = 21). We confirmed higher survival (p = 0.01), lower GVHD scores (p = 0.0028), and lower weight loss (p = 0.01) in PTCy-treated mice. Combined data from the two experiments (a total of 16 control and 17 PTCy mice) are presented in Figures 1A–1C. Median survival in control and PTCy-treated mice was 43 and 66 days, respectively (HR = 4.139; p < 0.0001). We also confirmed higher Treg (defined as $CD4^+CD25^+FOXP3^+$) frequencies in the peripheral blood on day 21 in PTCy-treated mice (median of 9.26 versus 2.75%, p = 0.0001) (Figure 1D). We next compared organ infiltration by human T cells in mice sacrificed on day 21 after hPBMC infusion and given (n = 19) or not (n = 18) PTCy. We observed lower human chimerism levels in the blood and the lungs, but not in the liver, BM, or spleen of PTCy-treated mice (Figure 1E). It should be stressed that human chimerism was lower in the BM than in the spleen or blood of each PTCy and control mice, in concordance with previous observations made in NSG mice infused with hPBMC without sub-lethal irradiation.[18] There was a higher frequency of Treg among $CD4^+$ T cells in all organs except for the BM (Figure 1F). Further, Treg from PTCy-treated mice exhibited higher FOXP3 (Figures 1G and 1H) and CD25 (Figure 1H) expression than those from control mice, reflecting a more suppressive Treg phenotype. This was associated with higher expression of IL-2 by $CD4^+$ T cells in PTCy-treated mice (Figure 1I). Comparing serum cytokine levels on day 28 after hPBMC infusion in another cohort of mice, we observed higher IL-2 but lower IFN-gamma and TNF-alpha serum concentrations in PTCy-treated mice (Figure 1J).

We next compared T-cell engraftment kinetics in control and PTCy-treated mice. We observed that human chimerism increased from day seven to day 21 and that this increase was higher in control than in PTCy-treated mice. Indeed, on day seven, human chimerism levels were higher in PTCy-treated mice (most probably reflecting the negative impact of cyclophosphamide on mouse hematopoiesis) while the opposite was seen on day 21 (reflecting the eradication of human proliferative T cells by PTCy; Figure S1A). Interestingly, Treg frequencies were higher in control mice on day seven, comparable in both groups on day 14, and higher in PTCy-treated mice on day 21 (Figure S1B). Proliferative $CD4^+$ and $CD8^+$ T cells were less frequent on day seven but more frequent on day 14 in PTCy-treated mice than in control mice (Figures S1C and S1D). As previously reported by other investigators,[23] there was an important decrease in the proportions of naive T cells (T_{naive}) among both $CD4^+$ and $CD8^+$ T-cell subsets from day 14 to day 21 after hPBMC infusion. In addition, among $CD4^+$ T cells, there were higher proportions of T_{naive} but lower proportions of effector T cells (TEFF) on days 14 and 21 in PTCy-treated than in control mice. Further, PTCy-treated mice had also higher proportions of central memory T cells (TCM) on day 14 (Figure S1E). Similarly, there were higher proportions of T_{naive} but lower proportions of TEFF on days 14 and 21 among $CD8^+$ T cells in PTCy-treated mice (Figure S1F). This observation is consistent with the higher proportion of IL-2 produced by $CD4^+$ T cells as T_{naive} and TCM produce more IL-2 than TEFF (Figure S1G). Thus, the Treg increase observed in PTCy-treated mice seems to be induced by higher IL-2 secretion by conventional T cells (Tconv). Finally, it should be stressed that while we consistently observed lower Treg frequencies

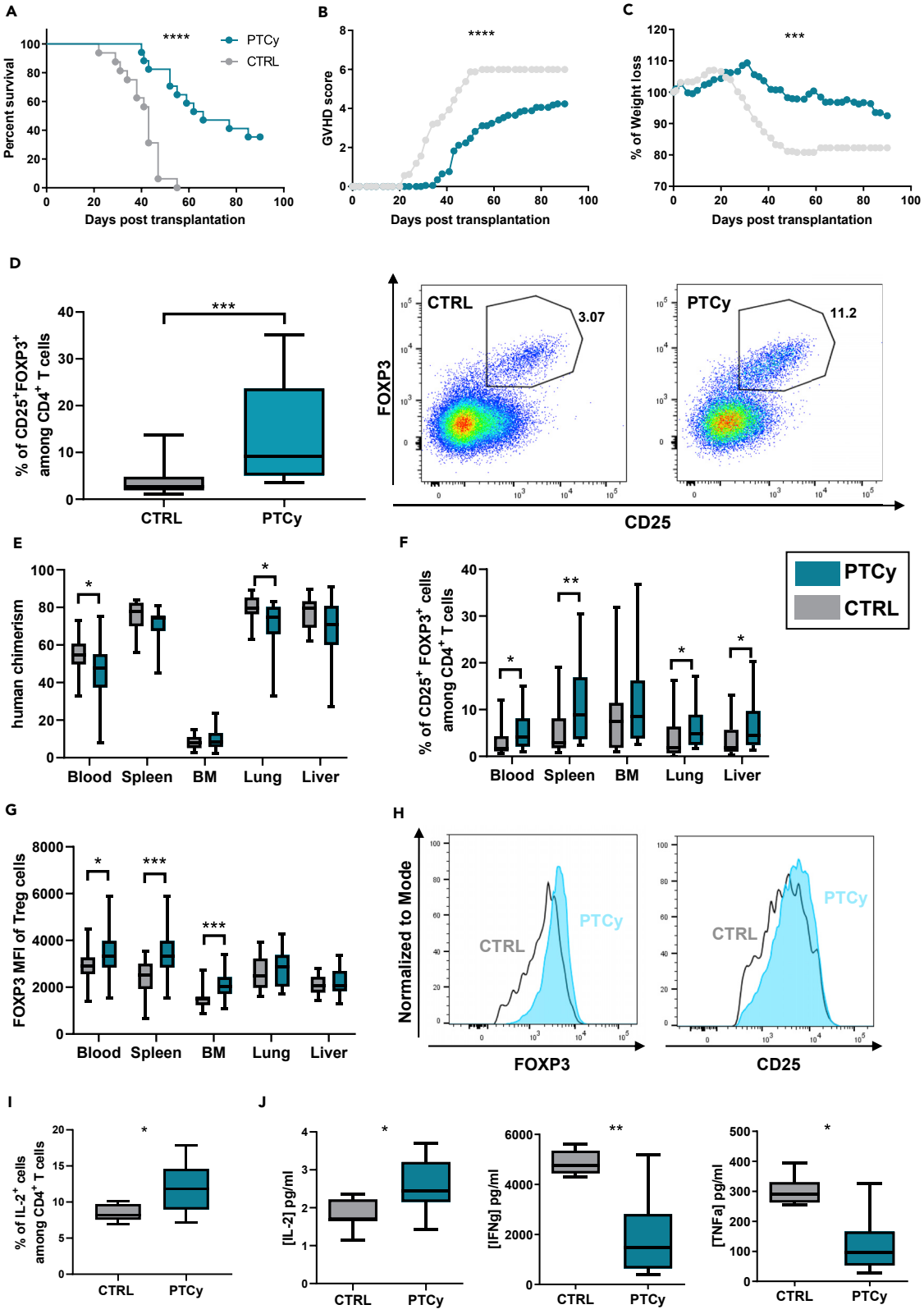
A
Percent survival
Days post transplantation
PTCy
CTRL
****
B
GVHD score
Days post transplantation
****
C
% of Weight loss
Days post transplantation
***
D
% of CD25+FOXP3+ among CD4+ T cells
CTRL
PTCy
***
FOXP3
CD25
3.07
11.2
E
human chimerism
Blood
Spleen
BM
Lung
Liver
F
% of CD25+ FOXP3+ cells among CD4+ T cells
PTCy
CTRL
G
FOXP3 MFI of Treg cells
H
Normalized to Mode
FOXP3
CD25
I
% of IL-2+ cells among CD4+ T cells
J
[IL-2] pg/ml
[IFNg] pg/ml
[TNFa] pg/ml

Figure 1. PTCy delays xGVHD

(A–D) In two independent cohorts NSG mice were transplanted with 2 × 10^7 hPBMC from two different healthy donors and were treated (blue, n = 17) or not (gray, n = 16) with PTCy (100 mg/kg) on day three. Mice were monitored for survival, GVHD score and weight loss, and flow cytometry analyses were performed on peripheral blood on day 21. (A) Comparison of survival curve, (B) xGVHD score, and (C) weight loss between control and PTCy-treated mice. Mice that reached a score of six were estimated to have terminal GVHD and were sacrificed. The final score for dead animals reaching the ethical limit score was kept in the dataset for the remaining time points (last observation carried forward).

(D) Comparison of Treg frequencies (defined as $CD25^+FOXP3^+$) among $CD4^+$ T cells and representative dot plot of concatenated $CD4^+$ T cells showing Treg frequencies in control and PTCy-treated mice.

(E–H) In two independent cohorts (CTRL, n = 18 and PTCy, n = 19), mice were sacrificed at day 21, and flow cytometry analyses were performed on peripheral blood, spleen, BM, lung, and liver. (E) Comparison of human chimerism (calculated as the ratio of human $CD45^+$ cells vs. murine + human $CD45^+$ cells). (F) Treg frequencies among $CD4^+$ T cells, and (G) FOXP3 MFI of Treg cells in xGVHD target organs. (H) Representative histogram of concatenated Treg from one cohort (CTRL, n 10 = and PTCy, n = 11) showing the expression of FOXP3 (left panel) and CD25 (right panel) between groups in the spleen.

(I and J) In an independent cohort (CTRL, n = 8 and PTCy, n = 8) human cytokine levels were analyzed on day 21 by flow cytometry and on day 28 by Luminex assay. (I) Comparison of IL-2^+ cells among $CD4^+$ T cells. (J) Comparison of indicated cytokine serum concentration. Data show median values with min to max for boxplots. (*p ≤ 0.05, **p < 0.01, ***p < 0.001, ****p < 0.0001). See also Figures S1 and S7.

on day 21 than on day 14, there were important variations among Treg frequencies observed between different hPBMC donors (Figure S1H).

Post-transplant administration of cyclophosphamide depletes proliferative ($KI67^+$) T cells including $KI67^+$ Treg

We next investigated the impact of PTCy on human T-cell subsets on day six after hPBMC infusion. In these experiments, mice were irradiated (2 Gy) on the day minus one, infused with 2 × 10^7 hPBMC on day zero, given or not a single dose of PTCy (100 mg/kg) on day three, and sacrificed on day six. Human chimerism was lower in the spleen but higher in the BM of PTCy-treated mice (Figures 2A and S2A). The latter was probably due to the toxicity of the cyclophosphamide on murine BM cells. In addition, there was a profound depletion of proliferating/activated T cells (i.e. $KI67^+$ and/or $CD25^+$) in both organs (Figures 2A, 2B, and S2A). In contrast, non-proliferating (i.e. $KI67^-$) BCL-2^+ T cells were not depleted by PTCy (Figures 2A, 2B, and S2A). Looking specifically at Treg subsets, we observed that PTCy depleted proliferative ($KI67^+$) splenic Treg but spared splenic $KI67^-$ Treg (Figures 2C and 2D). Interestingly, BM Tregs were not affected by PTCy (Figures S2B and S2C), possibly because of their lower KI67 and higher BCL-2 expression (Figure S2D). Finally, probably as a consequence of the important human T-cell count reduction by PTCy, there was a dramatic decrease in the IL-2 and IFN-gamma serum levels of PTCy-treated mice (Figure S2E).

To confirm our *in vivo* experiments showing that PTCy depletes proliferative Treg, we investigated the impact of mafosfamide (a cyclophosphamide analog with an endogenous cytotoxic activity) on Tconv and Treg *in vitro*. First, we observed that mafosfamide had no impact on total T-cell counts when T cells were not stimulated. Conversely, the numbers of T cells decreased in a concentration-dependent manner following exposure to mafosfamide when they were activated with CD3/CD28 beads (Figure S3A). Looking at $CD4^+$ T cells, both Tconv and Treg proliferated following activation with CD3/CD28 beads and the proportion of proliferative cells decreased following mafosfamide exposure (at either 4 or 8 μg/mL) in both Tconv and Treg (Figures S3B–S3D). This observation demonstrates that Treg are impacted by mafosfamide. In summary, these results support our *in vivo* findings that proliferating Treg are sensitive to cyclophosphamide.

Single-cell RNA-sequencing analyses reveal that post-transplant administration of cyclophosphamide depletes proliferative T cells overexpressing the mTor and aurora pathways but also Treg

To further assess the impact of PTCy on T cells in our GVHD model, we performed single-cell RNA-sequencing on human T cells isolated from the spleen of control and PTCy-treated mice on day six after hPBMC injection. Cell cycle phase analyses revealed that T cells from control mice were proliferating, with equivalent cell proportions observed in the G1 and G2M phases, and a smaller proportion of cells in the S phase (Figure 3A). Conversely, T cells from PTCy-treated mice were almost all in the G1 phase confirming that proliferative T cells were depleted by PTCy.

The clustering analysis evidenced two non-proliferative (naive T cells and cytotoxic T cells) and three proliferating (proliferating cytotoxic T cells, Treg (that were mostly proliferating) and proliferating helper T cells) cell groups (Figures 3B–3D, S4A, and S4B). Cytotoxic T cells were characterized by *CD8*, *NKG7*, *GZMB*, *PFRF1*, and *CCL5* expression (non-proliferative cytotoxic T cells) or similar expression plus *MKI67*

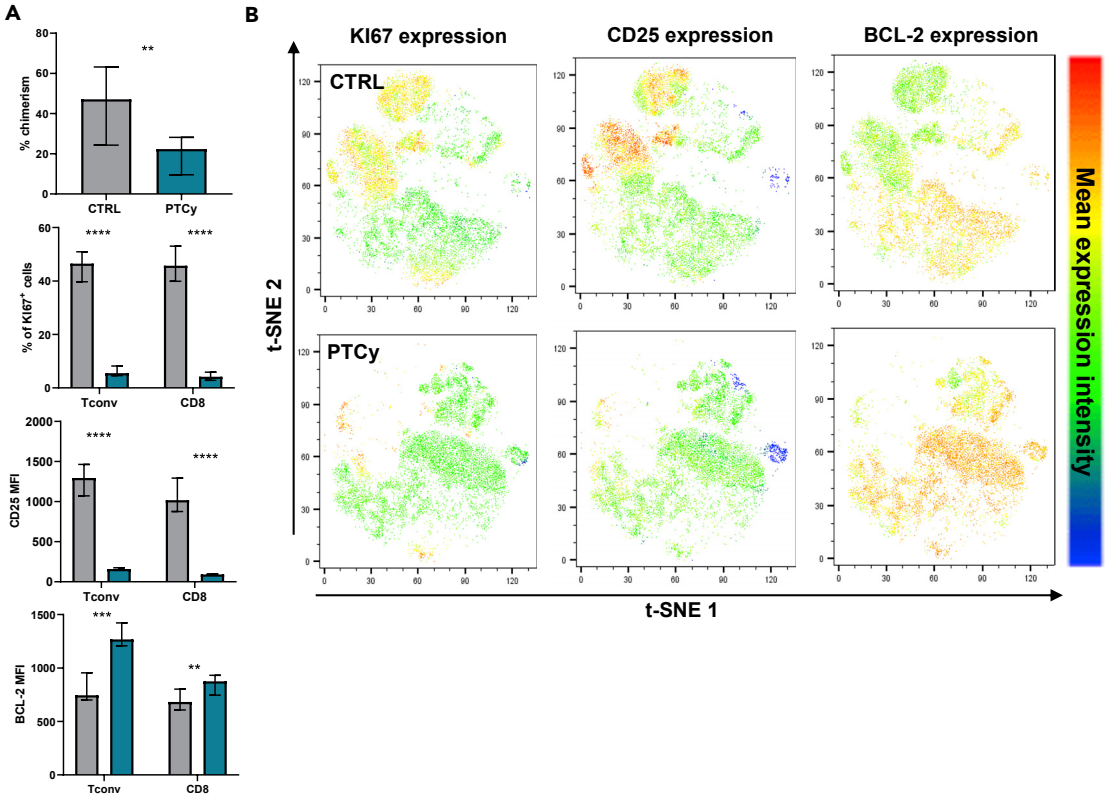
A
% chimerism
CTRL
PTCy
% of KI67+ cells
Tconv
CD8
CD25 MFI
BCL-2 MFI
B
KI67 expression
CD25 expression
BCL-2 expression
CTRL
PTCy
t-SNE 2
t-SNE 1
Mean expression intensity

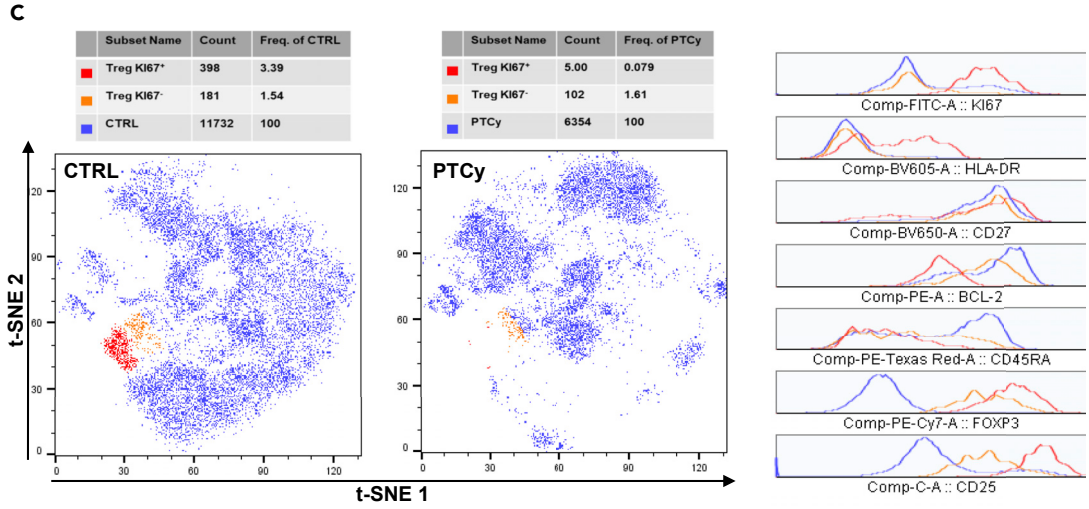
C
Subset Name | Count | Freq. of CTRL
Treg KI67+ | 398 | 3.39
Treg KI67- | 181 | 1.54
CTRL | 11732 | 100
Subset Name | Count | Freq. of PTCy
Treg KI67+ | 5.00 | 0.079
Treg KI67- | 102 | 1.61
PTCy | 6354 | 100
CTRL
PTCy
t-SNE 2
t-SNE 1
Comp-FITC-A :: KI67
Comp-BV605-A :: HLA-DR
Comp-BV650-A :: CD27
Comp-PE-A :: BCL-2
Comp-PE-Texas Red-A :: CD45RA
Comp-PE-Cy7-A :: FOXP3
Comp-C-A :: CD25

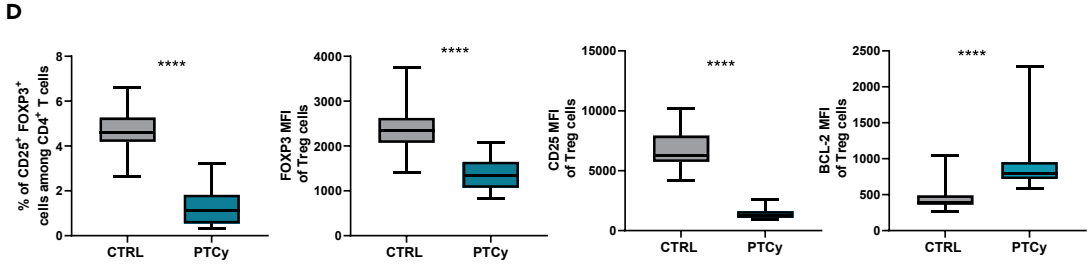
D
% of CD25+ FOXP3+ cells among CD4+ T cells
FOXP3 MFI of Treg cells
CD25 MFI of Treg cells
BCL-2 MFI of Treg cells
CTRL
PTCy

Figure 2. PTCy depletes proliferative (KI67$^+$) T cells and Treg

In four independent cohorts of mice, two Gy irradiated NSG mice were transplanted with 2 × 10^7 hPBMC from four different healthy donors and were treated (n = 21) or not (n = 18) with PTCy (100 mg/kg) on day three. Mice were sacrificed on day six for flow cytometry analyses on the spleen.

(A) Comparison of human chimerism, proliferative (i.e. KI67$^+$) cells, CD25, and BCL-2 expression among Tconv and CD8$^+$ T cells.

(B) Representative t-SNE of concatenated human CD45$^+$ cells from one mice cohort showing the expression of KI67 (left panel), CD25 (center), and BCL-2 (right panel) in the control group (n = 4) compared to the PTCy group (n = 4).

(C) Representative t-SNE analysis of concatenated CD4$^+$ T cells from one mice cohort showing Treg in the control group (n = 4) compared to the PTCy group (n = 4). Treg are divided into KI67$^+$ (red) and KI67$^-$ (orange).

(D) Comparison of Treg frequencies among CD4$^+$ T cells, comparison of FOXP3, CD25, and BCL-2 expression in Treg cells. Data show median values with min to max for boxplot or interquartile range for bar plot. (*p ≤ 0.05, **p < 0.01, ***p < 0.001, ****p < 0.0001). See also Figures S2 and S3.

expression (proliferative cytotoxic T cells). Proliferative helper T cells were characterized by *CD4* and *MKI67* expression and the absence of *FOXP3* expression (Figure 3C). Tregs were characterized by the expression of *FOXP3* and *CTLA4*. They also exhibited a high expression of other members of the "Treg gene signature" such as *IL2RA* and *TNFRSF1B* (TNFR2) (Figure S4C). Finally, naive T cells were defined based on a high *CCR7* expression and the absence of *MKI67* expression. Interestingly, while the five T-cell subpopulations were present in the control mice, mainly naive and non-proliferative cytotoxic T cells were present in PTCy-treated mice (Figures 3B–3D). Further, importantly, confirming flow cytometry analyses, Treg were extensively depleted by PTCy.

GSEA analyses comparing naive T cells from control and PTCy-treated mice revealed that cells exposed to cyclophosphamide had a higher expression of P53 and of apoptosis pathways with *BAX* and *BCL-2* being in the top 50 of the differentially expressed genes upregulated by PTCy (Figures 3E, S5A, and S5B). This demonstrates that PTCy, in addition to depleting proliferative T cells, also impacts the transcriptomic signature of naive non-proliferating T cells. We then performed further GSEA analyses on CD8$^+$ T cells comparing the transcriptome of non-proliferative to proliferative (which were depleted by PTCy) cytotoxic T-cell group. GVHD transcriptomic signatures such as Aurora kinase A and mTOR pathways[20,21] were overexpressed in the proliferative cytotoxic T cell group, evidencing that PTCy depleted mainly cells causing xGVHD (Figures 3F, S5C, and S5D).

T-cell V beta repertoire sequencing analyses demonstrate that post-transplant administration of cyclophosphamide eradicates the most xenoreactive clones

Since PTCy depleted proliferative T cells *in vivo*, we hypothesized that this might impact the T cell V beta (TCRVB) receptor repertoire diversity. Therefore, we performed TCRVB sequencing (TCR-seq) on T cells isolated from the pre-transplantation hPBMC (donor T cells) or from mice organs at day 21 post-transplantation (injected or not with PTCy at day three). As previously reported by our group,[21] the diversity of donor T cells at infusion was dramatically higher than in spleen or lung T cells (Figure 4A), demonstrating that xGVHD is mediated by a small fraction of T-cell clones expanding *in vivo* (most probably those recognizing mouse MHC by antigen mimicking).

While T-cell repertoires have been presumed to be almost entirely private, the development of high-throughput TCR sequencing has made clear that interindividual sharing of TCR clonotypes is more common than expected.[24,25] Interestingly, a low frequency of highly common clones (neonatal TCRs) in donors is a predictor of GVHD development in recipients.[26] Therefore, we wondered whether xGVHD could be mediated by clones more or less common between donors. Hence, we compared the overlap of identity between clonotypes present in donor PBMC reported herein and in a previous article of our group (unrelated donor).[21] The same comparison was made for T cells isolated from the spleen of NSG post-transplantation in both studies. In agreement with previous reports, the overlap between donor PBMC was close to 2% (1-8% similarity is typically observed).[24,25] The comparison of spleens showed that the overlap of T-cell identity was greatly reduced (~4-fold) in comparison to the one found in PBMC (Figure S6). In summary, these data suggest that GVHD in NSG mice is mediated by more private clones, in concordance with recent findings in humans.[26]

Next, we compared the control and treated animals and observed a less diverse repertoire in treated mice (Figure 4B). We hypothesized that the first and therefore most xenoreactive T-cell clones to react against mouse antigens are eliminated by PTCy in the early days of the treatment, sparing the less reactive ones. Following the expansion of these less reactive clones (which are expected to be mainly detected in treated mice by TCR-seq at day 21), this would result in two radically different T cell populations between control and treated animals. In concordance with this hypothesis, examining the identity of clonotypes between

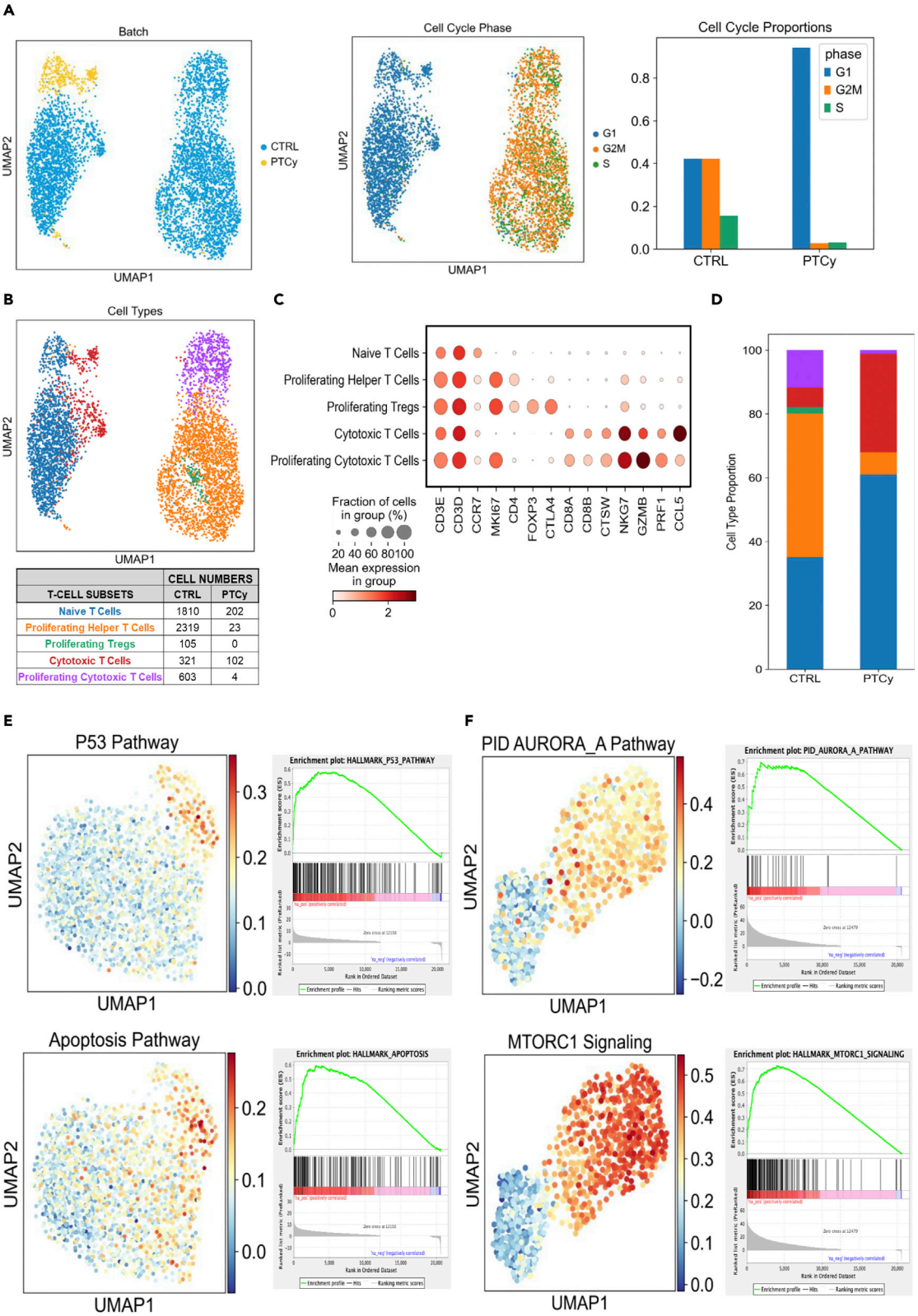

	CELL NUMBERS	
T-CELL SUBSETS	CTRL	PTCy
Naive T Cells	1810	202
Proliferating Helper T Cells	2319	23
Proliferating Tregs	105	0
Cytotoxic T Cells	321	102
Proliferating Cytotoxic T Cells	603	4

Figure 3. PTCy depletes proliferative T cells overexpressing the mTor and Aurora pathways but also Treg

NSG mice were transplanted with 2 × 10^7 hPBMC and were treated (n = 4) or not (n = 3) with PTCy (100 mg/kg) on day three. $CD3^+$ human T cells were isolated by immunomagnetic selection from mice spleen on day six and dead cell removal kit was used to exclude dead cells. Single-cell RNA-seq analysis was performed.

(A) UMAP visualization of cells from control (5275) and PTCy-treated mice (327) (left panel: blue = CTRL, orange = PTCy). UMAp visualization and proportions of G1, S, and G2M cell cycle phases in cells from control and PTCy-treated mice (center and right panel: blue = G1, orange = G2M, green = S).

(B–D) T cell subpopulations based on gene expression profile in control and PTCy-treated mice. (B) UMAP of five T-cells subpopulations: Naive (blue), proliferating helper (orange), proliferating Treg (green), cytotoxic (red), and proliferating cytotoxic (purple). (C) Heatmap showing specific marker gene expression in T-cell subpopulations. (D) Comparison of the proportion of each subpopulation in control and PTCy-treated mice.

(E) Enrichment plots of P53 (upper panel) and apoptosis (lower panel) pathways obtained from GSEA analysis contrasting naive cells from control and treated mice.

(F) Enrichment plots of mTOR (upper panel) and Aurora kinase A (lower panel) pathways obtained from GSEA analysis contrasting activated versus non-activated cytotoxic T cells in control mice. See also Figures S4 and S5.

both conditions, we found only a little overlap between the lungs of PTCy and control mice while there was a good correlation between the spleen and lungs of animals from the same condition (Figure 4C). Further, also supporting our hypothesis, a lower KI67 expression was found in T cells of treated mice on day seven (reflecting the inhibition of the most xenoreactive clones) but a greater KI67 expression was observed on day 14 (reflecting the unleashed proliferation of less xenoreactive clones spared by PTCy) (Figures S1C and S1D). Finally, we performed a differential expansion analysis of clonotypes between control animals and donor T cells. This provided the identity of significantly expanded clonotypes, which we defined as most xenoreactive ones, and those significantly contracted that we defined as bystanders. When comparing the overlap of identity between these two groups and clonotypes found in treated mice, we observed that bystanders were identified in significantly greater proportions in treated mice than xenoreactive clones, evidencing the elimination of xenoreactive clones by PTCy (Figure 4D). Next, we hypothesized that PTCy not only eliminated xenoreactive clones but also reduced the expansion of those having survived the treatment. To assess this, we identified the clonotypes significantly expanded in control or treated mice vs donor T cells. We observed that PTCy mice had significantly fewer expanded clonotypes than control animals among their whole repertoire (Figure 4E). Among the clonotypes significantly expanded in control mice (most xenoreactives), we selected those also detected in treated mice and compared their frequency between the two conditions (Figure 4F). We observed that these clonotypes were significantly less frequent in treated mice. Altogether, these results demonstrate that PTCy not only eradicates xenoreactive clones but also decreases their proliferation.

Low-dose IL-2 expands Treg following post-transplant administration of cyclophosphamide without providing additional graft-versus-host disease protection

It is now well established that IL-2 is the key homeostatic cytokine for Treg, preventing their apoptosis through MCL-1 expression.[27,28] Consequently, we performed additional experiments aimed at assessing whether the administration of low-dose of IL-2 could (1) protect proliferative Treg from PTCy, (2) expand Treg following PTCy, and/or (3) protect against xGVHD. Specifically, three groups of mice were injected with 2 × 10^7 hPBMC. The first group did not receive any treatment, the second group received PTCy (100 mg/kg i.p.) on day three, and the third received PTCy (100 mg/kg i.p.) on day three and low-dose IL-2 (25,000 IU/mouse/day i.p.)[29] from days two to 15 after hPBMC infusion.

A first observation was that IL-2 administration failed to protect proliferative Treg from PTCy (Figure 5A). Indeed, t-SNE analyses demonstrated less $KI67^+$ Treg on day seven in PTCy-treated and PTCy + IL-2-treated mice than in control mice, with no apparent differences between the two PTCy groups.

A second observation was that low-dose IL-2 expanded Treg following PTCy, increasing their frequencies among $CD4^+$ T cells and their absolute counts on days 14 and 21 after transplantation (Figures 5B and 5C). This was associated with higher pSTAT5 expression in Treg from the PTCy + IL-2 group at day 14 but also with higher pSTAT5 expression by $CD8^+$ T cells (Figure 5D).

A third observation was that, unfortunately, Treg expansion by low-dose IL-2 failed to prevent xGVHD, perhaps because low-dose IL-2 also fueled $CD25^+CD8^+$ T cells. On the contrary, GVHD scores tended to be higher and survival lower in PTCy + IL-2 mice than in PTCy-treated mice (Figure 5E).

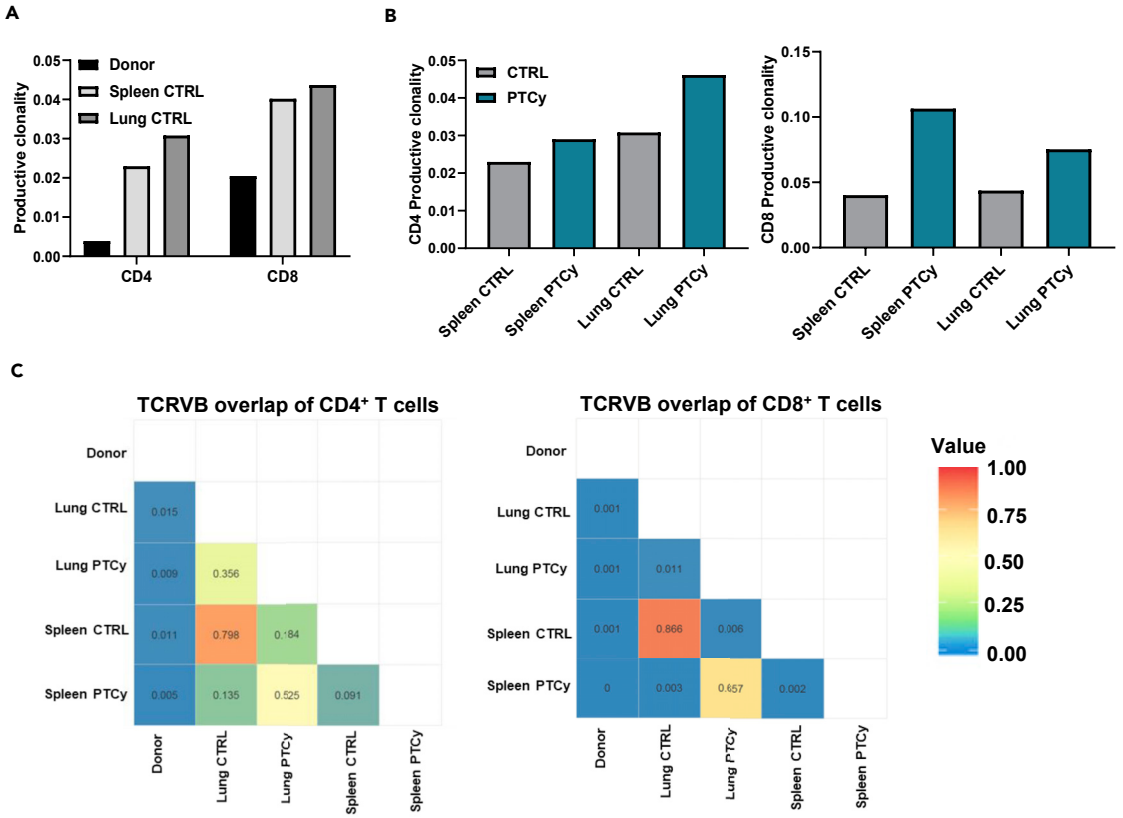
A
Productive clonality
Donor
Spleen CTRL
Lung CTRL
CD4
CD8
B
CD4 Productive clonality
CD8 Productive clonality
CTRL
PTCy
Spleen CTRL
Spleen PTCy
Lung CTRL
Lung PTCy
C
TCRVB overlap of CD4+ T cells
TCRVB overlap of CD8+ T cells
Value
1.00
0.75
0.50
0.25
0.00
Donor
Lung CTRL
Lung PTCy
Spleen CTRL
Spleen PTCy
D
% Clonotypes shared with treated sample
CTRL UP
CTRL DOWN
E
% Upregulated clonotypes vs donor T cells
CTRL
PTCy
CD4 spleen
CD4 lung
CD8 spleen
CD8 lung
F
Xenoreactive CD8 clonotypes in the spleen
Xenoreactive CD4 clonotypes in the spleen
Xenoreactive CD8 clonotypes in the lung
Xenoreactive CD4 clonotypes in the lung
Frequency %
CTRL
PTCy

Figure 4. PTCy eradicates the most xenoreactive clones

NSG mice were injected with 2 × 10^7 hPBMC and treated (n = 10) or not (n = 10) with PTCy (100 mg/kg) on day three. Mice were sacrificed on day 21 for harvesting $CD4^+$ and $CD8^+$ T cells from the spleen and lungs. DNA was extracted and TCRVB sequencing analysis was performed.

(A) Productive clonality (higher clonality indicates a less diverse repertoire) of $CD4^+$ and $CD8^+$ T cells between the donor (before infusion to mice) and spleen/lungs from control mice.

(B) Productive clonality of $CD4^+$ and $CD8^+$ T cells from the spleen and lung between control and PTCy-treated mice.

(C) Heatmap of clonotypes overlap between samples calculated by Morista index for $CD4^+$ T cells (left panel) and $CD8^+$ T cells (right panel).

(D) Proportion of $CD4^+$ and $CD8^+$ clonotypes upregulated (Up, = xenoreactive clonotypes) and clonotypes downregulated (Down, = bystanders) in control found in PTCy-treated mice.

(E) Proportion of $CD4^+$ and $CD8^+$ clonotypes upregulated in spleen/lungs from control vs donor or from treated vs donor.

(F) Frequency of $CD4^+$ and $CD8^+$ xenoreactive clonotypes from the spleen/lungs shared between control and PTCy-treated mice. Data show median values with min to max for boxplot. (*p ≤ 0.05, **p < 0.01, ***p < 0.001, ****p < 0.0001). See also Figure S6.

Treg are not mandatory for xenogeneic graft-versus-host disease attenuation by post-transplant administration of cyclophosphamide

We investigated whether Treg were required for xGVHD attenuation by PTCy. Therefore, we compared GVHD and immune parameters of mice transplanted with unmanipulated hPBMC (CTRL, n = 7) vs mice transplanted with CD25-depleted hPBMC and treated (n = 10) or not (n = 10) with PTCy. We observed that untreated mice given CD25-depleted hPBMC had exacerbated xGVHD in comparison to control mice, as previously observed by other group of investigators[30,31] (Figure S7A). Furthermore, as expected, Treg frequencies were extensively lower in mice given CD25-depleted hPBMC than in those receiving unmanipulated hPBMC (Figures S7B and S7C). Importantly, we observed that PTCy still significantly mitigated xGVHD in mice infused with CD25-depleted hPBMC, demonstrating that Treg were not mandatory for xGVHD mitigation by PTCy (HR for survival 2.5, p = 0.019). However, it should be stressed that none of the 10 mice given CD25-depleted hPBMC and PTCy survived beyond day 90, while two control mice were given unmanipulated hPBMC survived. Accordingly, PTCy-treated mice given CD25-depleted hPBMC had significantly shorter survival than PTCy-treated mice transplanted with unmanipulated hPBMC in 3 independent cohorts including a total of 25 mice (median of 42 vs 66 days, p = 0.0004) (Figure S7D).

Taken together these results demonstrate that Treg are not mandatory for GVHD attenuation by PTCy. Nevertheless, it should be stressed that CD25-depletion exacerbated xGVHD in both control and PTCy-treated mice with the best survival being observed in mice receiving PTCy and unmanipulated hPBMC.

Post-transplant administration of cyclophosphamide depletes natural killer cells

Given that a recent systems biology analysis suggested an important role for NK cells in GvL effects in the setting of PTCy-based GVHD prophylaxis,[17] we assessed the impact of PTCy on NK cells. Since human NK cells poorly engraft in NSG mice, we performed these experiments in NSG-IL-15 mice. Indeed, we reasoned that IL-15 could support NK cell engraftment in our mouse model, as observed when mice are infused with hematopoietic stem cells.[32] Further, in this mouse strain model, human T- (particularly $CD8^+$) cells are stimulated by IL-15 and do not depend only on IL-2 produced by activated T cells to proliferate (as in the classical NSG mouse model). In agreement with observations made in classical NSG mice, we observed that PTCy significantly decreased xGVHD and increased Treg proportions at day 30 also in NSG-IL15 mice (Figures 6A and 6B). Importantly, at day 10 we observed a significant depletion of NK cells (as well as of proliferative T cells) in PTCy-treated mice, demonstrating that NK cells were susceptible to PTCy *in vivo* (Figure 6C). Unfortunately, the frequencies of NK cells on day 21 were low in both groups, precluding the analysis of the long-term impact of PTCy on NK cells (Figure 6D).

Post-transplant administration of cyclophosphamide does not abrogate graft-versus-leukemia effects

Since we observed that PTCy ameliorated xGVHD and depleted NK cells we investigated whether PTCy would also abrogate the GvL effect. We addressed this important question in NSG-HLA-A2/HHD mice (a strain of NSG mice, that express the human HLA-A0201 in addition to mouse MHC) in order to have some common antigens between the mouse organs and the human AML cell line THP-1, as previously reported by our group.[21,33] All mice were injected i.v. with THP-1 cells transfected with the luciferase gene on days zero and five. The reason for the first THP-1 injection was to have leukemic cells on board when PTCy was administered (mimicking clinical situations in which minimal residual disease or active leukemia would be present at the time of allo-HCT) and because of the sensitivity of THP-1 cells to

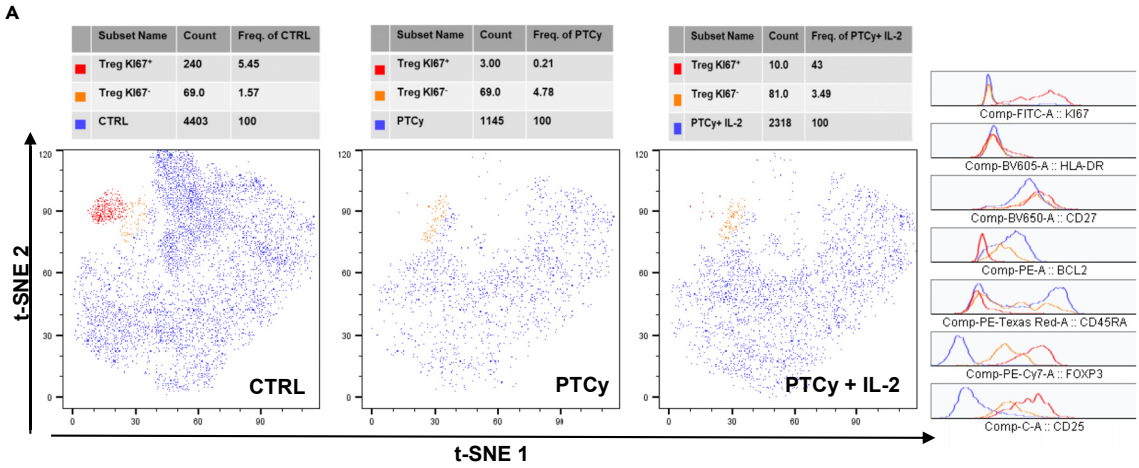
A
Subset Name | Count | Freq. of CTRL
Treg KI67+ | 240 | 5.45
Treg KI67- | 69.0 | 1.57
CTRL | 4403 | 100
Subset Name | Count | Freq. of PTCy
Treg KI67+ | 3.00 | 0.21
Treg KI67- | 69.0 | 4.78
PTCy | 1145 | 100
Subset Name | Count | Freq. of PTCy+ IL-2
Treg KI67+ | 10.0 | 43
Treg KI67- | 81.0 | 3.49
PTCy+ IL-2 | 2318 | 100
t-SNE 2
t-SNE 1
CTRL
PTCy
PTCy + IL-2
Comp-FITC-A :: KI67
Comp-BV605-A :: HLA-DR
Comp-BV650-A :: CD27
Comp-PE-A :: BCL2
Comp-PE-Texas Red-A :: CD45RA
Comp-PE-Cy7-A :: FOXP3
Comp-C-A :: CD25

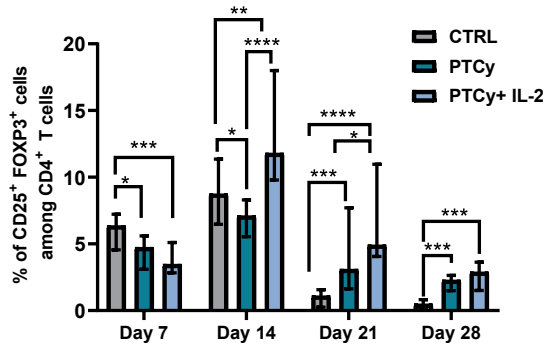
B
% of CD25+ FOXP3+ cells among CD4+ T cells
CTRL
PTCy
PTCy+ IL-2
Day 7
Day 14
Day 21
Day 28

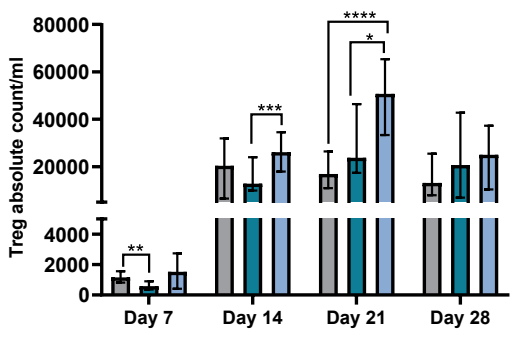
C
Treg absolute count/ml
Day 7
Day 14
Day 21
Day 28

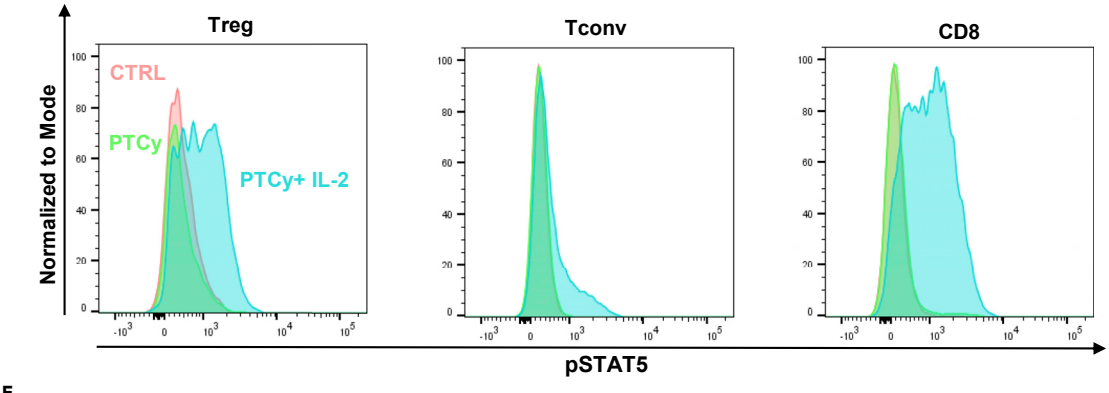
D
Treg
Tconv
CD8
CTRL
PTCy
PTCy+ IL-2
Normalized to Mode
pSTAT5

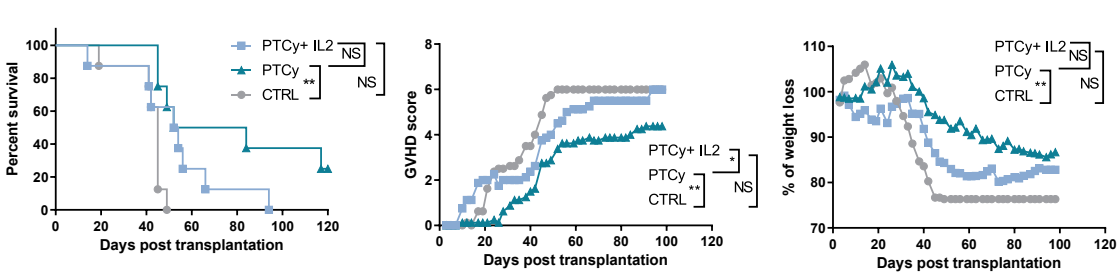
E
Percent survival
Days post transplantation
PTCy+ IL2
PTCy
CTRL
NS
GVHD score
% of weight loss

Figure 5. IL-2 expands Treg following PTCy without providing additional GVHD protection

In two independent cohorts, NSG mice were transplanted with 2 × 10^7 hPBMC from two different healthy donors and were treated with PTCy alone or PTCy in combination with human recombinant IL-2 25,000 IU/mice (CTRL, n = 16, PTCy n = 16, PTCy + IL-2 = 17) from day two to day 15. Mice were monitored for survival, GVHD score, weight loss, and flow cytometry analyses were performed on peripheral blood.

(A) Representative t-SNE of concatenated $CD4^+$ T cells from one mouse cohort showing Treg cells on day seven in control (n = 8, left panel), PTCy (n = 8, center panel) and PTCy + IL-2 (n = 8, right panel) group. Treg are divided into $KI67^+$ (red) and $KI67^-$ (orange).

(B and C) Comparison of Treg frequencies among $CD4^+$ T cells and (C) Treg count per mL at different time points.

(D) Representative histogram of concatenated Treg (left panel), Tconv (center panel), $CD8^+$ T cells (right panel) from one mouse cohort showing the pSTAT5 expression on day 14 between the three groups (CTRL = pink, PTCy = green, PTCy + IL-2 = blue).

(E) Survival (left panel), GVHD score (center panel), and weight loss (right panel) of one mouse cohort (CTRL, n = 8, PTCy n = 8, PTCy + IL-2 = 8). Mice that reached a score of six were estimated to have terminal GVHD and were sacrificed. Data show median values with interquartile range for bar plot. (*$p \leq 0.05$, **$p < 0.01$, ***$p < 0.001$, ****$p < 0.0001$).

cyclophosphamide. Four groups of mice were compared, a group of mice given only THP-1 cells, a second group given THP-1 cells and PTCy on day three, a third group given THP-1 cells and hPBMC from a non-HLA-A2 donor, and a fourth group given THP-1 cells, PTCy, and hPBMC from the same non-HLA-A2 donor. The best survival was observed in THP-1 + PTCy + hPBMC mice (Figure 7A). Bioluminescence analysis revealed that none of the THP-1 + hPBMC mice had detectable tumors while THP-1 + PTCy + hPBMC mice had detectable tumors but to a lesser extent than THP-1 only or THP-1 + PTCy mice (Figure 7B). We concluded from this experiment that, although decreased, GvL effects were not abrogated by PTCy.

DISCUSSION

Although PTCy is increasingly used as GVHD prophylaxis, how it prevents GVHD as well as its impact on GvL effects remain debated. Specifically, the role of Treg on GVHD mitigation by PTCy has been intensively studied.[13,14,34] Here, we extensively studied the mechanisms of GVHD prevention by PTCy in three humanized mouse models of GVHD. Several important observations were made.

First, we confirmed that PTCy prevented xGVHD in NSG mice infused with hPBMC. We also observed such a protective effect of PTCy in NSG-HLA-A2-HDD mice, a model in which GVHD is induced by both xenogeneic and allogeneic reactions when hPBMC from non-HLA-A2 donors are infused,[21,35] and in NSG-IL15 mice, a model in which infused human ($CD8^+$) T cells are supported independently of IL-2.[36] Accordingly, serum levels of IFN-gamma and TNF-alpha were significantly decreased by PTCy in the NSG mouse model, as generally observed when successful anti-GVHD approaches are investigated.[22,33]

An important observation of our study was that Treg were not required for GVHD protection by PTCy. Indeed, we observed that PTCy attenuated xGVHD in mice given CD25-depleted hPBMC while mouse peripheral blood analyses confirmed dramatically low Treg numbers on days seven and 14 in NSG mice injected with CD25-depleted hPBMC. These results are in contrast with those previously reported by Ganguly et al. in mouse-to-mouse models of experimental GVHD in which GVHD scores of mice given $CD4^+CD25^{high}$-depleted grafts before PTCy were slightly lower but statistically similar to mice given $CD4^+CD25^{high}$-depleted grafts without PTCy.[13] Here, we hypothesize that this discrepancy could be ascribed to either fundamental differences between human and mouse immunology (particularly in regard of Treg biology[37]), or perhaps to insufficient statistical power in the Ganguly et al. study to detect a statistically significant impact of PTCy in mice given $CD4^+CD25^{high}$-depleted. However, in concordance with Ganguly et al. observations, we did observe a lower survival in PTCy mice given CD25-depleted hPBMC in comparison to PTCy mice given unmodified hPBMC. This demonstrates that Treg depletion exacerbates xGVHD and suggests.

The observation that Treg were not mandatory for GVHD reduction by PTCy prompted us to revisit the impact of PTCy on Treg. *In vitro* experiments demonstrated that activated/proliferating Treg were highly susceptible to mafosfamide (a cyclophosphamide analog). These observations were confirmed *in vivo* by the demonstration that PTCy depleted $KI67^+$ Treg by flow cytometry experiments and by single-cell RNA-seq analyses. The latter identified only the fraction of "proliferative" Treg from the spleen at day six in control mice. These proliferative Treg were virtually absent at day six in the spleen of PTCy mice. These results are in contrast to prior observations by Kanakry et al. who proposed that Treg were resistant to PTCy following allogeneic hematopoietic cell transplantation because they acquired the expression of ALDH, as demonstrated by the authors in *in vitro* mixed lymphoid reactions.[14]

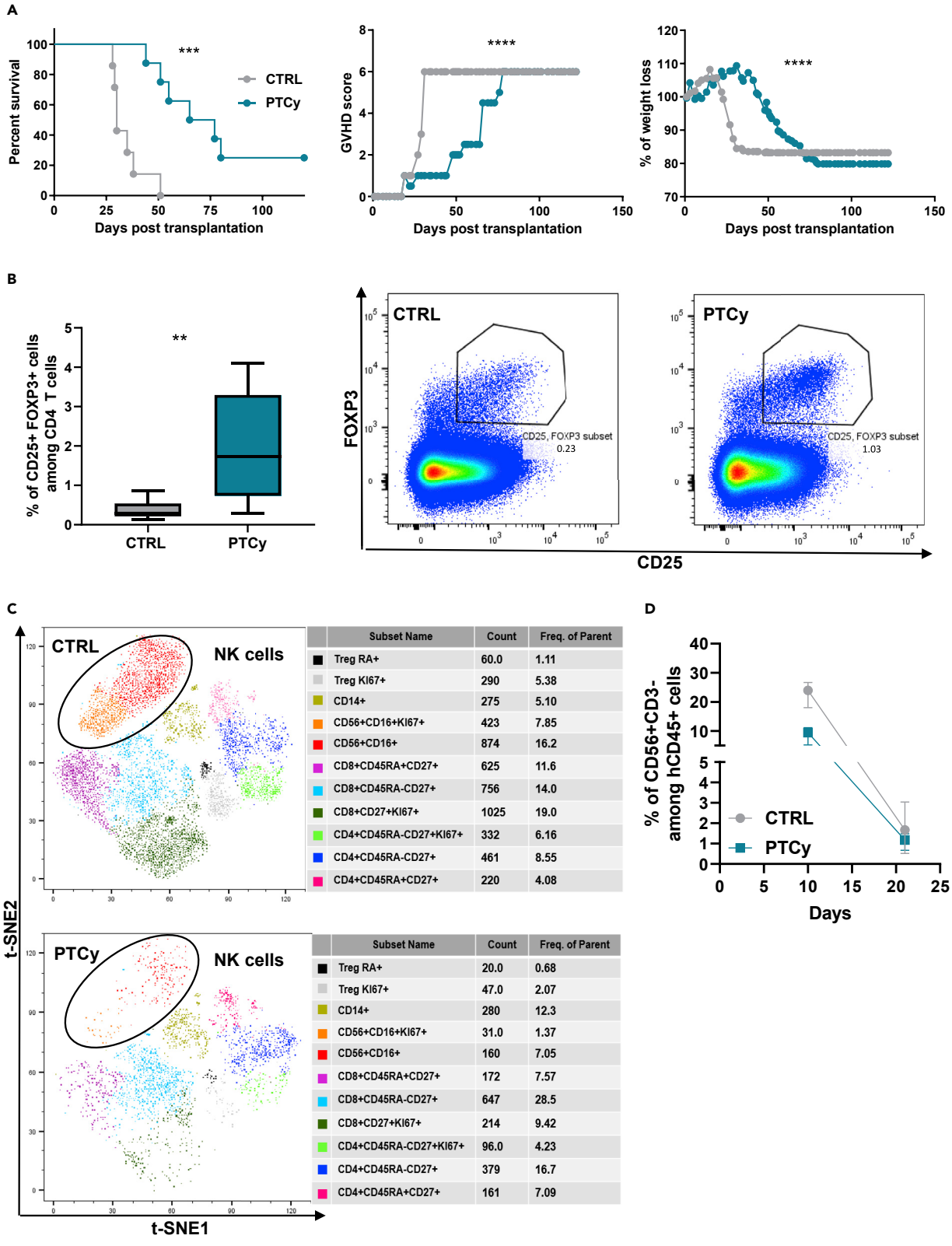

Subset Name	Count	Freq. of Parent
Treg RA+	60.0	1.11
Treg KI67+	290	5.38
CD14+	275	5.10
CD56+CD16+KI67+	423	7.85
CD56+CD16+	874	16.2
CD8+CD45RA+CD27+	625	11.6
CD8+CD45RA-CD27+	756	14.0
CD8+CD27+KI67+	1025	19.0
CD4+CD45RA-CD27+KI67+	332	6.16
CD4+CD45RA-CD27+	461	8.55
CD4+CD45RA+CD27+	220	4.08

Subset Name	Count	Freq. of Parent
Treg RA+	20.0	0.68
Treg KI67+	47.0	2.07
CD14+	280	12.3
CD56+CD16+KI67+	31.0	1.37
CD56+CD16+	160	7.05
CD8+CD45RA+CD27+	172	7.57
CD8+CD45RA-CD27+	647	28.5
CD8+CD27+KI67+	214	9.42
CD4+CD45RA-CD27+KI67+	96.0	4.23
CD4+CD45RA-CD27+	379	16.7
CD4+CD45RA+CD27+	161	7.09

Figure 6. PTCy depletes NK cells

(A and B) NSG-IL15 mice were transplanted with 2 × 10^7 hPBMC and were treated (blue, n = 8) or not (gray, n = 8) with PTCy (100 mg/kg) on day three. Mice were monitored for survival, GVHD score, weight loss and flow cytometry analyses were performed on blood around day 30.

(C) NSG-IL-15 mice were transplanted with 1 × 10^7 hPBMC and were treated (n = 4) or not (n = 4) with PTCy (100 mg/kg) on day three. Flow cytometry analyses on peripheral blood were performed on day 10.

(A) Comparison of the survival curve, xGVHD score, and weight loss between control and PTCy-treated mice. Mice that reached a score of six were estimated to have terminal GVHD and were sacrificed.

(B) Comparison of Treg frequencies among $CD4^+$ T cells (left panel), a representative dot plot of Treg cells from control and PTCy-treated mice (right panel).

(C) Representative t-SNE of concatenated human $CD45^+$ cells in control (n = 4) and PTCy-treated mice (n = 4). NK cells are divided into two populations, proliferating NK cells ($KI67^+$, orange) and non-proliferating NK cells (red).

(D) Evolution of the percentages of NK cells in the peripheral blood in NSG-IL15 mice injected with 10 × 10^6 hPBMC. Data show median values with min to max for boxplot. (*p ≤ 0.05, **p < 0.01, ***p < 0.001, ****p < 0.0001).

The low IL-2 serum levels combined with the low FOXP3 and low CD25 levels in Treg from PTCy-treated mice on day seven prompted us to investigate whether the administration of low doses of IL-2 could attenuate xGVHD. We observed that low-dose IL-2 was very efficient at promoting the expansion of Treg that survived PTCy administration. In addition to inducing higher Treg proportions, IL-2 also increased their expression of CD25 and pSTAT5. These findings are consistent with what has been observed in chronic patients with GVHD benefiting from low-dose IL-2 therapy.[38,39] Unfortunately, low doses of IL-2 also promoted $CD8^+$ T cells which acquired high levels of pSTAT5 and, consequently, xGVHD was not improved. This is consistent with prior reports showing that activated $CD8^+$ T cells and Treg could compete for IL-2 in inflammatory conditions,[40,41] and with an elegant study by Perol et al. which showed that the administration of low-dose IL-2 expanded Treg in NSG mice infused with hPBMC but did not improve survival (with a trend to the contrary),[29] mirroring what we observed in our PTCy experiments.

Our results also evidenced the depletion of proliferative Tconv and proliferative $CD8^+$ T cells by PTCy. These results are in concordance with those reported by Adhikary et al. who observed that PTCy (33 mg/kg at days 3 and 4) reduced the proportion of alloreactive T cells (defined as carboxyfluorescein succinimidyl ester $(CFSE)^{Low}$ T cells) six days after the injection of 2 × 10^7 CFSE-labelled hPBMC in NSG mice.[34] We further observed an accumulation of BCL-2-expressing T cells. Single-cell RNA-seq confirmed the depletion of proliferative T cells (including proliferative Treg as mentioned above) by PTCy. Importantly, the proliferative cytotoxic T-cell subpopulation depleted by PTCy overexpressed the AURORA kinase A and mTOR pathways which have been previously associated with a GVHD transcriptomic signature in non-human primates and in the NSG mouse model.[20,21,42] Interestingly, we also noticed an overexpression of the P53 and apoptosis pathways by PTCy in T cells that survived the exposition to the drug. Consequently, higher proportions of naive T cells and TCM were observed in PTCy-treated mice following hPBMC infusion. This is significant since naive $CD4^+$ T cells were the most IL-2-secreting cells in flow cytometry experiments on day 21.

Analyses of TCRVB repertoire confirmed our previous observation that a limited fraction of the T-cell population expands in NSG mice to mediate GVHD.[21] In addition, comparing baseline and post-infusion T-cell repertoire between two PBMC donors revealed a particularly low overlap post-hPBMC infusion (even lower than between PBMC donor at baseline) showing that the clonotypes expanding in NSG mice are more private than those detected in PBMCs from healthy donors. Interestingly, this "private" response to xenogeneic antigens reflects what has been reported by other investigators for cytomegalovirus (CMV) infection as shared antigen exposure to CMV leads to fewer shared TCRβ clones, indicative of a largely private response to major viral antigenic exposure.[24] Such private reaction to identical antigens (either vaccination or HIV infection) has even been demonstrated between identical twins, suggesting that it is not linked to pre-established genetic parameters.[43,44] Further, importantly, we observed that PTCy significantly reduced the frequency of multiple xenoreactive T-cell clones, in agreement with the inhibition of highly proliferative T-cell populations observed by other methods. Interestingly, this result contrasts with a previous report showing that PTCy does not impact the TCRVB clonality in myeloablative allo-HCT recipients vs patients treated with methotrexate and a calcineurin inhibitor[45], this discrepancy could be due to the antiproliferative activity of their control treatments, similar to the effect of PTCy on the TCRVB repertoire.

Finally, using our xenogeneic/allogeneic humanized model of GVHD we investigated the impact of PTCy on GvL effects. Indeed, the impact of PTCy-based GVHD prophylaxis in patients with active disease at transplantation has remained debated and there are concerns that PTCy could not only prevent GVHD

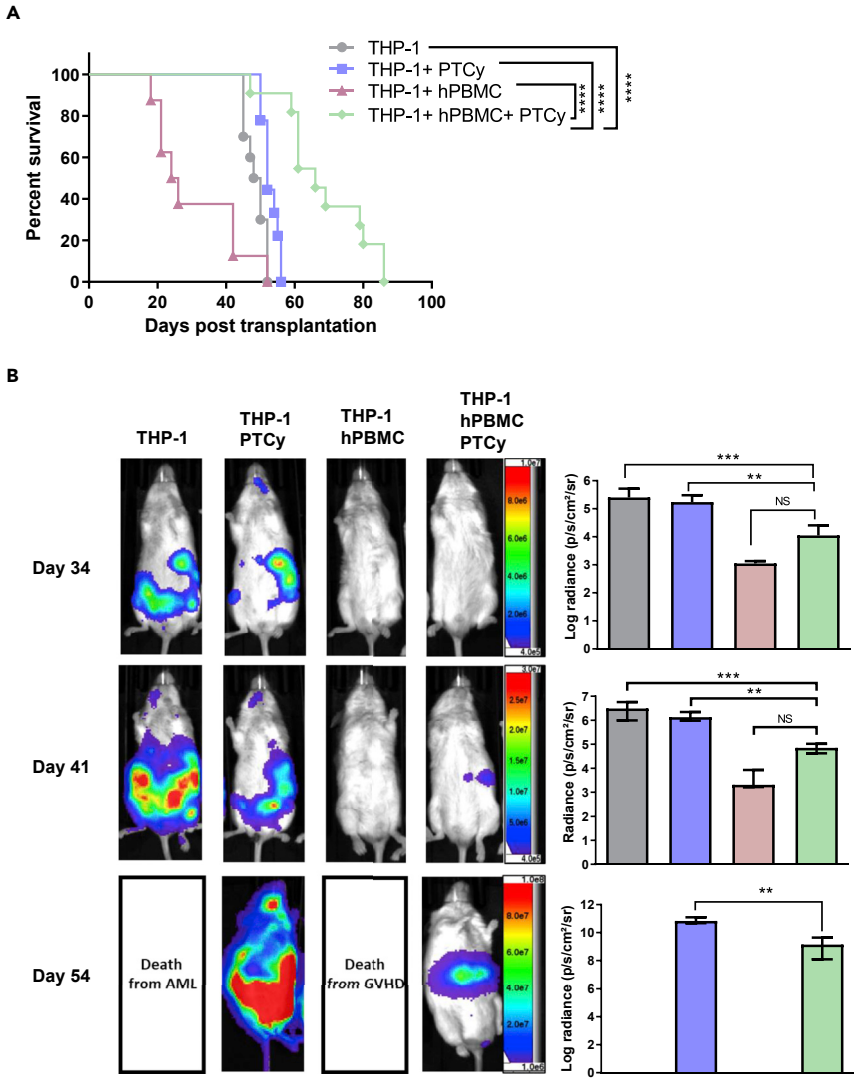

Figure 7. PTCy does not abrogate GvL effects

NSG-HLA-A2/HDD mice were transplanted with 3 × 10^6 THP-1-luc$^+$ cells on day zero together or not with 2 × 10^7 hPBMC also on day zero. Mice were either treated or not with PTCy 100 mg/kg on day three and all mice received a second injection of 2 × 10^6 THP-1-luc$^+$ cells on day five (THP-1, gray, n = 10 – THP-1+PTCy, blue, n = 9 – THP-1+hPBMC, red, n = 8 – THP-1+hPBMC + PTCy, green, n = 11). Survival and bioluminescence were monitored.

(A) survival curve between the four groups.

(B) Images follow-up of one representative mouse from each group are shown with photon flux (photons/sec) measured from the ventral view (region of interest was drawn over the entire body of each mouse). THP-1+hPBMC mice do not develop tumors, photon flux observed corresponding to signal background. The right panels show the comparison of bioluminescence between groups. Data show median values with interquartile range (*$p < 0.05$, **$p < 0.005$, ***$p < 0.0005$).

but also abrogate GvL effects in this context. We observed that although PTCy reduced GvL effects, it did not abrogate them. Consequently, the best survival was observed in mice treated by PTCy (which were somewhat protected from GVHD and still exhibited some GvL effects) while mice not infused with hPBMC died of leukemia, and mice infused by hPBMC but not given PTCy died most probably because of GVHD. These observations are compatible with recent observations reported by investigators from the acute leukemia working party of the European Society for Blood and Marrow Transplantation who demonstrated that GVHD occurrence did not correlate with GvL effects in patients given PTCy-based GVHD prophylaxis.[46] The slightly lower GvL effects observed after PTCy in our model might also be due to the destruction of NK cells by PTCy since IL-12-activated human NK cells have been shown to have an anti-leukemic activity

in NSG mice bearing THP-1 cells,[47] while significant concentrations of human IL-12 are present in NSG mice infused with hPBMC.[48] Supporting this hypothesis, a recent study in allo-HCT recipients given PTCy-based GVHD prophylaxis demonstrated lower relapse incidence and better overall survival in patients with NK cell counts >50.5 cells/μL on day 28 after transplantation.[17] Further, in that study, among HLA-haploidentical transplant recipients, patients who experienced early relapse displayed a loss of inflammatory gene signatures in their NK cells.

In conclusion, extensive analyses of mechanisms of xGVHD prevention by PTCy revealed that cyclophosphamide works mainly by the depletion of proliferative xenoreactive T cells. Despite proliferative Treg are also depleted by PTCy, Treg proportion was more abundant and Treg expressed higher levels of FOXP3 and CD25 in PTCy than in control mice 21 days after hPBMC injection. This was due to higher IL-2 levels in PTCy-treated mice, which in contrast had lower levels of IFN-gamma and TNF-alpha, two cytokines highly correlated with xGVHD severity.

Limitations of the study

We acknowledge some limitations in our study. First, the humanized GVHD models used in this study were not fully humanized since only the T-cell compartment was stably engrafted following PBMC injection, even in NSG-IL-15 mice. Secondly, given that the xGVHD reactions were mediated against many MHC antigens we had to assume that most proliferative T cells at the time of GVHD were xenoreactive T cells (or xenoreactive or alloreactive T cells in the experiments with the NSG-HLA-A2/HHD mice). However, repertoire analyses clearly demonstrated that only a minority of TCR clones expanded after hPBMC infusion in NSG mice while there were no correlations between clonotype frequencies at injection and those recovered in the mice 21 days after the injection suggesting that most proliferative T cells in these humanized models were indeed xenoreactive.

STAR★METHODS

Detailed methods are provided in the online version of this paper and include the following:

- KEY RESOURCES TABLE
- RESOURCE AVAILABILITY
  - Lead contact
  - Materials availability
  - Data and code availability
- EXPERIMENTAL MODEL AND SUBJECT DETAILS
  - Mice
  - Primary cell culture
- METHOD DETAILS
  - Induction of xGVHD and PTCy administration
  - Flow cytometry
  - Serum cytokine levels
  - CFSE proliferation assay
  - TCR repertoire diversity
  - Single cell RNA-Seq
  - GvL effects and bioluminescence imaging
- QUANTIFICATION AND STATISTICAL ANALYSIS

SUPPLEMENTAL INFORMATION

Supplemental information can be found online at https://doi.org/10.1016/j.isci.2023.106085.

ACKNOWLEDGMENTS

CR, J Co, LC, and BV are Televie Research Fellow, CB is a Medical Doctor Applicant for an MSc and a Ph.D., GE is a Postdoctoral Researcher and FB is a senior research associate at the Fund for Scientific Research (F.R.S.–FNRS) Belgium. The study was funded by grants from the Stichting Tegen Kanker - Fondation contre le Cancer Belgium (grant # FAF-C/2016/844), by the Fund for Scientific Research (F.R.S.–FNRS) Belgium (grant # T.0016.20), by the University of Liège, as well as by the Leon Fredericq fund and the Anti-Cancer Center from the University of Liège. We are grateful to Sandra Ormenese, Raafat Stephan,

and Céline Vanwinge from the Imaging and Flow Cytometry Platform and to Latifa Karim and Arnaud Lavergne from the Genomic platform of the GIGA for their help with flow cytometry/transcriptomic analyses.

AUTHOR CONTRIBUTIONS

Design of the project: FB, CR, GE.

Inputs on the project design: SS, JCa, YB.

Mouse experiments: CR, JCo, SD, LC, CB, BV.

Flow cytometry experiments and interpretations: CR, GE, FB.

Single-seq RNA seq analyses: MCK, CR, JCa.

TCRVB repertoire analyses: GE.

Figures: CR, MCK, GE.

Ms writing: FB, CR.

Ms editing and approval: all authors.

DECLARATION OF INTERESTS

The authors declare no competing interests.

Received: September 30, 2022
Revised: December 12, 2022
Accepted: January 25, 2023
Published: January 31, 2023

REFERENCES

1. Zeiser, R., and Blazar, B.R. (2017). Acute graft-versus-host disease - biologic process, prevention, and therapy. N. Engl. J. Med. *377*, 2167–2179. https://doi.org/10.1056/NEJMra1609337.

2. Socié, G., and Ritz, J. (2014). Current issues in chronic graft-versus-host disease. Blood *124*, 374–384. https://doi.org/10.1182/blood-2014-01-514752.

3. Weiden, P.L., Sullivan, K.M., Flournoy, N., Storb, R., and Thomas, E.D.; Seattle Marrow Transplant Team (1981). Antileukemic effect of chronic graft-versus-host disease: contribution to improved survival after allogeneic marrow transplantation. N. Engl. J. Med. *304*, 1529–1533. https://doi.org/10.1056/NEJM198106183042507.

4. Baron, F., Maris, M.B., Sandmaier, B.M., Storer, B.E., Sorror, M., Diaconescu, R., Woolfrey, A.E., Chauncey, T.R., Flowers, M.E.D., Mielcarek, M., et al. (2005). Graft-versus-tumor effects after allogeneic hematopoietic cell transplantation with nonmyeloablative conditioning. J. Clin. Oncol. *23*, 1993–2003. https://doi.org/10.1200/JCO.2005.08.136.

5. Baron, F., Labopin, M., Niederwieser, D., Vigouroux, S., Cornelissen, J.J., Malm, C., Vindelov, L.L., Blaise, D., Janssen, J.J.W.M., Petersen, E., et al. (2012). Impact of graft-versus-host disease after reduced-intensity conditioning allogeneic stem cell transplantation for acute myeloid leukemia: a report from the Acute Leukemia Working Party of the European group for blood and marrow transplantation. Leukemia *26*, 2462–2468. https://doi.org/10.1038/leu.2012.135.

6. Storb, R., Antin, J.H., and Cutler, C. (2010). Should methotrexate plus calcineurin inhibitors be considered standard of care for prophylaxis of acute graft-versus-host disease? Biol. Blood Marrow Transplant. *16*, S18–S27. https://doi.org/10.1016/j.bbmt.2009.10.016.

7. Baron, F., Mohty, M., Blaise, D., Socié, G., Labopin, M., Esteve, J., Ciceri, F., Giebel, S., Gorin, N.C., Savani, B.N., et al. (2017). Anti-thymocyte globulin as graft-versus-host disease prevention in the setting of allogeneic peripheral blood stem cell transplantation: a review from the Acute Leukemia Working Party of the European Society for Blood and Marrow Transplantation. Haematologica *102*, 224–234. https://doi.org/10.3324/haematol.2016.148510.

8. Kanakry, C.G., Fuchs, E.J., and Luznik, L. (2016). Modern approaches to HLA-haploidentical blood or marrow transplantation. Nat. Rev. Clin. Oncol. *13*, 132. https://doi.org/10.1038/nrclinonc.2015.234.

9. Brissot, E., Labopin, M., Moiseev, I., Cornelissen, J.J., Meijer, E., Van Gorkom, G., Rovira, M., Ciceri, F., Griskevicius, L., Blaise, D., et al. (2020). Post-transplant cyclophosphamide versus antithymocyte globulin in patients with acute myeloid leukemia in first complete remission undergoing allogeneic stem cell transplantation from 10/10 HLA-matched unrelated donors. J. Hematol. Oncol. *13*, 87. https://doi.org/10.1186/s13045-020-00923-0.

10. Dholaria, B., Labopin, M., Sanz, J., Ruggeri, A., Cornelissen, J., Labussière-Wallet, H., Blaise, D., Forcade, E., Chevallier, P., Grassi, A., et al. (2021). Allogeneic hematopoietic cell transplantation with cord blood versus mismatched unrelated donor with post-transplant cyclophosphamide in acute myeloid leukemia. J. Hematol. Oncol. *14*, 76. https://doi.org/10.1186/s13045-021-01086-2.

11. Shaw, B.E., Jimenez-Jimenez, A.M., Burns, L.J., Logan, B.R., Khimani, F., Shaffer, B.C., Shah, N.N., Mussetter, A., Tang, X.-Y., McCarty, J.M., et al. (2021). National marrow donor program-sponsored multicenter, phase II trial of HLA-mismatched unrelated donor bone marrow transplantation using

post-transplant cyclophosphamide. J. Clin. Oncol. *39*, 1971–1982. https://doi.org/10.1200/JCO.20.03502.

12. Baron, F., Labopin, M., Tischer, J., Ciceri, F., Raiola, A.M., Blaise, D., Sica, S., Vydra, J., Fanin, R., Stölzel, F., et al. (2022). HLA-haploidentical transplantation for relapsed/refractory AML: better LFS with BM than with PBSC in patients ≥ 55 years of age. Am. J. Hematol. *97*, 1065–1074. https://doi.org/10.1002/ajh.26627.

13. Ganguly, S., Ross, D.B., Panoskaltsis-Mortari, A., Kanakry, C.G., Blazar, B.R., Levy, R.B., and Luznik, L. (2014). Donor CD4+ Foxp3+ regulatory T cells are necessary for posttransplantation cyclophosphamide-mediated protection against GVHD in mice. Blood *124*, 2131–2141. https://doi.org/10.1182/blood-2013-10-525873.

14. Kanakry, C.G., Ganguly, S., Zahurak, M., Bolaños-Meade, J., Thoburn, C., Perkins, B., Fuchs, E.J., Jones, R.J., Hess, A.D., and Luznik, L. (2013). Aldehyde dehydrogenase expression drives human regulatory T cell resistance to posttransplantation cyclophosphamide. Sci. Transl. Med. *5*, 211ra157. https://doi.org/10.1126/scitranslmed.3006960.

15. Zhao, C., Bartock, M., Jia, B., Shah, N., Claxton, D.F., Wirk, B., Rakszawski, K.L., Nickolich, M.S., Naik, S.G., Rybka, W.B., et al. (2022). Post-transplant cyclophosphamide alters immune signatures and leads to impaired T cell reconstitution in allogeneic hematopoietic stem cell transplant. J. Hematol. Oncol. *15*, 64. https://doi.org/10.1186/s13045-022-01287-3.

16. Massoud, R., Gagelmann, N., Fritzsche-Friedland, U., Zeck, G., Heidenreich, S., Wolschke, C., Ayuk, F., Christopeit, M., and Kröger, N. (2022). Comparison of immune reconstitution between anti-T-lymphocyte globulin and post-transplant cyclophosphamide as acute graft-versus-host disease prophylaxis in allogeneic myeloablative peripheral blood stem cell transplantation. Haematologica *107*, 857–867. https://doi.org/10.3324/haematol.2020.271445.

17. McCurdy, S.R., Radojcic, V., Tsai, H.-L., Vulic, A., Thompson, E., Ivcevic, S., Kanakry, C.G., Powell, J.D., Lohman, B., Adom, D., et al. (2022). Signatures of GVHD and relapse after post-transplant cyclophosphamide revealed by immune profiling and machine learning. Blood *139*, 608–623. https://doi.org/10.1182/blood.2021013054.

18. King, M.A., Covassin, L., Brehm, M.A., Racki, W., Pearson, T., Leif, J., Laning, J., Fodor, W., Foreman, O., Burzenski, L., et al. (2009). Human peripheral blood leucocyte non-obese diabetic-severe combined immunodeficiency interleukin-2 receptor gamma chain gene mouse model of xenogeneic graft-versus-host-like disease and the role of host major histocompatibility complex. Clin. Exp. Immunol. *157*, 104–118. https://doi.org/10.1111/j.1365-2249.2009.03933.x.

19. Kawasaki, Y., Sato, K., Hayakawa, H., Takayama, N., Nakano, H., Ito, R., Mashima, K., Oh, I., Minakata, D., Yamasaki, R., et al. (2018). Comprehensive analysis of the activation and proliferation kinetics and effector functions of human lymphocytes, and antigen presentation capacity of antigen-presenting cells in xenogeneic graft-versus-host disease. Biol. Blood Marrow Transplant. *24*, 1563–1574. https://doi.org/10.1016/j.bbmt.2018.04.016.

20. Furlan, S.N., Watkins, B., Tkachev, V., Flynn, R., Cooley, S., Ramakrishnan, S., Singh, K., Giver, C., Hamby, K., Stempora, L., et al. (2015). Transcriptome analysis of GVHD reveals aurora kinase A as a targetable pathway for disease prevention. Sci. Transl. Med. *7*, 315ra191. https://doi.org/10.1126/scitranslmed.aad3231.

21. Ehx, G., Somja, J., Warnatz, H.-J., Ritacco, C., Hannon, M., Delens, L., Fransolet, G., Delvenne, P., Muller, J., Beguin, Y., et al. (2018). Xenogeneic graft-versus-host disease in humanized NSG and NSG-HLA-A2/HHD mice. Front. Immunol. *9*, 1943. https://doi.org/10.3389/fimmu.2018.01943.

22. Ehx, G., Ritacco, C., Hannon, M., Dubois, S., Delens, L., Willems, E., Servais, S., Drion, P., Beguin, Y., and Baron, F. (2021). Comprehensive analysis of the immunomodulatory effects of rapamycin on human T cells in graft-versus-host disease prophylaxis. Am. J. Transplant. *21*, 2662–2674. https://doi.org/10.1111/ajt.16505.

23. Ali, N., Flutter, B., Sanchez Rodriguez, R., Sharif-Paghaleh, E., Barber, L.D., Lombardi, G., and Nestle, F.O. (2012). Xenogeneic graft-versus-host-disease in NOD-scid IL-2Rγnull mice display a T-effector memory phenotype. PLoS One *7*, e44219. https://doi.org/10.1371/journal.pone.0044219.

24. Johnson, S.A., Seale, S.L., Gittelman, R.M., Rytlewski, J.A., Robins, H.S., and Fields, P.A. (2021). Impact of HLA type, age and chronic viral infection on peripheral T-cell receptor sharing between unrelated individuals. PLoS One *16*, e0249484. https://doi.org/10.1371/journal.pone.0249484.

25. Soto, C., Bombardi, R.G., Kozhevnikov, M., Sinkovits, R.S., Chen, E.C., Branchizio, A., Kose, N., Day, S.B., Pilkinton, M., Gujral, M., et al. (2020). High frequency of shared clonotypes in human T cell receptor repertoires. Cell Rep. *32*, 107882. https://doi.org/10.1016/j.celrep.2020.107882.

26. Trofimov, A., Brouillard, P., Larouche, J.-D., Séguin, J., Laverdure, J.-P., Brasey, A., Ehx, G., Roy, D.-C., Busque, L., Lachance, S., et al. (2022). Two types of human TCR differentially regulate reactivity to self and non-self antigens. iScience *25*, 104968. https://doi.org/10.1016/j.isci.2022.104968.

27. Pierson, W., Cauwe, B., Policheni, A., Schlenner, S.M., Franckaert, D., Berges, J., Humblet-Baron, S., Schönefeldt, S., Herold, M.J., Hildeman, D., et al. (2013). Antiapoptotic Mcl-1 is critical for the survival and niche-filling capacity of Foxp3(+) regulatory T cells. Nat. Immunol. *14*, 959–965. https://doi.org/10.1038/ni.2649.

28. Liston, A., and Gray, D.H.D. (2014). Homeostatic control of regulatory T cell diversity. Nat. Rev. Immunol. *14*, 154–165. https://doi.org/10.1038/nri3605.

29. Pérol, L., Martin, G.H., Maury, S., Cohen, J.L., and Piaggio, E. (2014). Potential limitations of IL-2 administration for the treatment of experimental acute graft-versus-host disease. Immunol. Lett. *162*, 173–184. https://doi.org/10.1016/j.imlet.2014.10.027.

30. Mutis, T., van Rijn, R.S., Simonetti, E.R., Aarts-Riemens, T., Emmelot, M.E., van Bloois, L., Martens, A., Verdonck, L.F., and Ebeling, S.B. (2006). Human regulatory T cells control xenogeneic graft-versus-host disease induced by autologous T cells in RAG2-/-gammac-/- immunodeficient mice. Clin. Cancer Res. *12*, 5520–5525. https://doi.org/10.1158/1078-0432.CCR-06-0035.

31. Hippen, K.L., Merkel, S.C., Schirm, D.K., Sieben, C.M., Sumstad, D., Kadidlo, D.M., McKenna, D.H., Bromberg, J.S., Levine, B.L., Riley, J.L., et al. (2011). Massive ex vivo expansion of human natural regulatory T cells (T(regs)) with minimal loss of in vivo functional activity. Sci. Transl. Med. *3*, 83ra41. https://doi.org/10.1126/scitranslmed.3001809.

32. Aryee, K.-E., Burzenski, L.M., Yao, L.-C., Keck, J.G., Greiner, D.L., Shultz, L.D., and Brehm, M.A. (2022). Enhanced development of functional human NK cells in NOD-scid-IL2rg(null) mice expressing human IL15. Faseb. J. *36*, e22476. https://doi.org/10.1096/fj.202200045R.

33. Ehx, G., Fransolet, G., de Leval, L., D'Hondt, S., Lucas, S., Hannon, M., Delens, L., Dubois, S., Drion, P., Beguin, Y., et al. (2017). Azacytidine prevents experimental xenogeneic graft-versus-host disease without abrogating graft-versus-leukemia effects. OncoImmunology *6*, e1314425. https://doi.org/10.1080/2162402X.2017.1314425.

34. Adhikary, S.R., Cuthbertson, P., Nicholson, L., Bird, K.M., Sligar, C., Hu, M., O'Connell, P.J., Sluyter, R., Alexander, S.I., and Watson, D. (2021). Post-transplant cyclophosphamide limits reactive donor T cells and delays the development of graft-versus-host disease in a humanized mouse model. Immunology *164*, 332–347. https://doi.org/10.1111/imm.13374.

35. Courtois, J., Ritacco, C., Dubois, S., Canti, L., Vandenhove, B., Seidel, L., Daulne, C., Caers, J., Servais, S., Beguin, Y., et al. (2021). Itacitinib prevents xenogeneic GVHD in humanized mice. Bone Marrow Transplant. *56*, 2672–2681. https://doi.org/10.1038/s41409-021-01363-1.

36. Covington, M., He, X., Scuron, M., Li, J., Collins, R., Juvekar, A., Shin, N., Favata, M., Gallagher, K., Sarah, S., et al. (2020). Preclinical characterization of itacitinib (INCB039110), a novel selective inhibitor of JAK1, for the treatment of inflammatory diseases. Eur. J. Pharmacol. *885*, 173505. https://doi.org/10.1016/j.ejphar.2020.173505.

37. Ziegler, S.F. (2006). FOXP3: of mice and men. Annu. Rev. Immunol. *24*, 209–226. https://doi.org/10.1146/annurev.immunol.24.021605.090547.

38. Matsuoka, K.i., Koreth, J., Kim, H.T., Bascug, G., McDonough, S., Kawano, Y., Murase, K., Cutler, C., Ho, V.T., Alyea, E.P., et al. (2013). Low-dose interleukin-2 therapy restores regulatory T cell homeostasis in patients with chronic graft-versus-host disease. Sci. Transl. Med. *5*, 179ra43. https://doi.org/10.1126/scitranslmed.3005265.

39. Ritacco, C., Ehx, G., Grégoire, C., Daulne, C., Willems, E., Servais, S., Beguin, Y., and Baron, F. (2021). High proportion of terminally differentiated regulatory T cells after allogeneic hematopoietic stem cell transplantation. Bone Marrow Transplant. *56*, 1828–1841. https://doi.org/10.1038/s41409-021-01221-0.

40. Humblet-Baron, S., Franckaert, D., Dooley, J., Bornschein, S., Cauwe, B., Schönefeldt, S., Bossuyt, X., Matthys, P., Baron, F., Wouters, C., and Liston, A. (2016). IL-2 consumption by highly activated CD8 T cells induces regulatory T-cell dysfunction in patients with hemophagocytic lymphohistiocytosis. J. Allergy Clin. Immunol. *138*, 200–209.e8. https://doi.org/10.1016/j.jaci.2015.12.1314.

41. Abraham, S., Pahwa, R., Ye, C., Choi, J.-G., Pahwa, S., Jaggaiahgari, S., Raut, A., Chen, S., Manjunath, N., and Shankar, P. (2012). Long-term engraftment of human natural T regulatory cells in NOD/SCID IL2rγc(null) mice by expression of human IL-2. PLoS One *7*, e51832. https://doi.org/10.1371/journal.pone.0051832.

42. Betts, B.C., Veerapathran, A., Pidala, J., Yang, H., Horna, P., Walton, K., Cubitt, C.L., Gunawan, S., Lawrence, H.R., Lawrence, N.J., et al. (2017). Targeting Aurora kinase A and JAK2 prevents GVHD while maintaining Treg and antitumor CTL function. Sci. Transl. Med. *9*, eaai8269. https://doi.org/10.1126/scitranslmed.aai8269.

43. Pogorelyy, M.V., Minervina, A.A., Touzel, M.P., Sycheva, A.L., Komech, E.A., Kovalenko, E.I., Karganova, G.G., Egorov, E.S., Komkov, A.Y., Chudakov, D.M., et al. (2018). Precise tracking of vaccine-responding T cell clones reveals convergent and personalized response in identical twins. Proc. Natl. Acad. Sci. USA *115*, 12704–12709. https://doi.org/10.1073/pnas.1809642115.

44. Yu, X.G., Lichterfeld, M., Williams, K.L., Martinez-Picado, J., and Walker, B.D. (2007). Random T-cell receptor recruitment in human immunodeficiency virus type 1 (HIV-1)-specific CD8+ T cells from genetically identical twins infected with the same HIV-1 strain. J. Virol. *81*, 12666–12669. https://doi.org/10.1128/JVI.01450-07.

45. Kanakry, C.G., Coffey, D.G., Towlerton, A.M.H., Vulic, A., Storer, B.E., Chou, J., Yeung, C.C.S., Gocke, C.D., Robins, H.S., O'Donnell, P.V., et al. (2016). Origin and evolution of the T cell repertoire after posttransplantation cyclophosphamide. JCI Insight *1*, e86252. https://doi.org/10.1172/jci.insight.86252.

46. Shimoni, A., Labopin, M., Angelucci, E., Blaise, D., Ciceri, F., Koc, Y., Gülbas, Z., Diez-Martin, J.L., Bruno, B., Castagna, L., et al. (2022). The association of graft-versus-leukemia effect and graft-versus host disease in haploidentical transplantation with post-transplant cyclophosphamide for AML. Bone Marrow Transplant. *57*, 384–390. https://doi.org/10.1038/s41409-021-01493-6.

47. Cany, J., van der Waart, A.B., Spanholtz, J., Tordoir, M., Jansen, J.H., van der Voort, R., Schaap, N.M., and Dolstra, H. (2015). Combined IL-15 and IL-12 drives the generation of CD34(+)-derived natural killer cells with superior maturation and alloreactivity potential following adoptive transfer. OncoImmunology *4*, e1017701. https://doi.org/10.1080/2162402X.2015.1017701.

48. Pyo, K.H., Kim, J.H., Lee, J.-M., Kim, S.E., Cho, J.S., Lim, S.M., and Cho, B.C. (2019). Promising preclinical platform for evaluation of immuno-oncology drugs using Hu-PBL-NSG lung cancer models. Lung Cancer *127*, 112–121. https://doi.org/10.1016/j.lungcan.2018.11.035.

49. Hannon, M., Lechanteur, C., Lucas, S., Somja, J., Seidel, L., Belle, L., Bruck, F., Baudoux, E., Giet, O., Chantillon, A.-M., et al. (2014). Infusion of clinical-grade enriched regulatory T cells delays experimental xenogeneic graft-versus-host disease. Transfusion *54*, 353–363. https://doi.org/10.1111/trf.12279.

50. SIMPSON, E.H. (1949). Measurement of diversity. Nature *163*, 688. https://doi.org/10.1038/163688a0.

51. DeWitt, W.S., Emerson, R.O., Lindau, P., Vignali, M., Snyder, T.M., Desmarais, C., Sanders, C., Utsugi, H., Warren, E.H., McElrath, J., et al. (2015). Dynamics of the cytotoxic T cell response to a model of acute viral infection. J. Virol. *89*, 4517–4526. https://doi.org/10.1128/JVI.03474-14.

52. Benjamini, Y., and Hochberg, Y. (1995). Controlling the False Discovery rate: a practical and powerful approach to multiple testing. J. Roy. Stat. Soc. B *57*, 289–300. https://doi.org/10.1111/j.2517-6161.1995.tb02031.x.

53. Zheng, G.X.Y., Terry, J.M., Belgrader, P., Ryvkin, P., Bent, Z.W., Wilson, R., Ziraldo, S.B., Wheeler, T.D., McDermott, G.P., Zhu, J., et al. (2017). Massively parallel digital transcriptional profiling of single cells. Nat. Commun. *8*, 14049. https://doi.org/10.1038/ncomms14049.

54. Wolf, F.A., Angerer, P., and Theis, F.J. (2018). SCANPY: large-scale single-cell gene expression data analysis. Genome Biol. *19*, 15. https://doi.org/10.1186/s13059-017-1382-0.

55. Satija, R., Farrell, J.A., Gennert, D., Schier, A.F., and Regev, A. (2015). Spatial reconstruction of single-cell gene expression data. Nat. Biotechnol. *33*, 495–502. https://doi.org/10.1038/nbt.3192.

56. Korsunsky, I., Millard, N., Fan, J., Slowikowski, K., Zhang, F., Wei, K., Baglaenko, Y., Brenner, M., Loh, P.-R., and Raychaudhuri, S. (2019). Fast, sensitive and accurate integration of single-cell data with Harmony. Nat. Methods *16*, 1289–1296. https://doi.org/10.1038/s41592-019-0619-0.

57. Becht, E., McInnes, L., Healy, J., Dutertre, C.-A., Kwok, I.W.H., Ng, L.G., Ginhoux, F., and Newell, E.W. (2018). Dimensionality reduction for visualizing single-cell data using UMAP. Nat. Biotechnol. *37*, 38–44. https://doi.org/10.1038/nbt.4314.

58. Traag, V.A., Waltman, L., and van Eck, N.J. (2019). From Louvain to Leiden: guaranteeing well-connected communities. Sci. Rep. *9*, 5233. https://doi.org/10.1038/s41598-019-41695-z.

59. Tirosh, I., Izar, B., Prakadan, S.M., Wadsworth, M.H., 2nd, Treacy, D., Trombetta, J.J., Rotem, A., Rodman, C., Lian, C., Murphy, G., et al. (2016). Dissecting the multicellular ecosystem of metastatic melanoma by single-cell RNA-seq. Science *352*, 189–196. https://doi.org/10.1126/science.aad0501.

60. Subramanian, A., Tamayo, P., Mootha, V.K., Mukherjee, S., Ebert, B.L., Gillette, M.A., Paulovich, A., Pomeroy, S.L., Golub, T.R., Lander, E.S., and Mesirov, J.P. (2005). Gene set enrichment analysis: a knowledge-based approach for interpreting genome-wide expression profiles. Proc. Natl. Acad. Sci. USA *102*, 15545–15550. https://doi.org/10.1073/pnas.0506580102.

STAR★METHODS

KEY RESOURCES TABLE

REAGENT or RESOURCE	SOURCE	IDENTIFIER
Antibodies		
BV510 Mouse Anti-Human CD45	BD Biosciences	Cat#563204;RRID:AB_2738067
CD45 Monoclonal Antibody (30-F11), PE-Cyanine5, eBioscience™	Thermo Fisher Scientific	Cat#15-0451-81; RRID:AB_468751
CD3 APC	BD Biosciences	Cat#345767; RRID:AB_2833003
CD4 Monoclonal Antibody (RPA-T4), eFluor™ 450	Thermo Fisher Scientific	Cat#48-0049-42; RRID:AB_1272057
PE/Cyanine7 anti-human CD8 Antibody	BioLegend	Cat#344712; RRID:AB_2044008
APC-Cy™7 Mouse Anti-Human CD8	BD Biosciences	Cat# 557834; RRID:AB_396892)
PE Mouse Anti-Human CD8	BD Biosciences	Cat# 555635; RRID:AB_395997
FITC Mouse Anti-Human CD16	BD Biosciences	Cat# 555406; RRID:AB_395806
PE-CF594 Mouse Anti-Human CD45RA	BD Biosciences	Cat# 562326; RRID:AB_11152953
Brilliant Violet 785™ anti-human CD45RA Antibody	BioLegend	Cat# 304140; RRID:AB_2563816
BV650 Mouse Anti-Human CD27	BD Biosciences	Cat# 563228; RRID:AB_2744352
CD62L (L-Selectin) Monoclonal Antibody (DREG-56 (DREG56)), APC-eFluor™ 780, eBioscience™	Thermo Fisher Scientific	Cat# 47-0629-42; RRID:AB_1582224
BB515 Mouse Anti-Human CD62L	BD Biosciences	Cat# 565037; RRID:AB_2744437
CD14 Monoclonal Antibody (61D3), eFluor™ 450, eBioscience™	Thermo Fisher Scientific	Cat# 48-0149-42; RRID:AB_1272050
BUV395 Mouse Anti-Human CD25	BD Biosciences	Cat# 564034; RRID:AB_2738556
APC-R700 Mouse Anti-Human CD56	BD Biosciences	Cat# 565140
Brilliant Violet 605™ anti-human HLA-DR Antibody	BioLegend	Cat# 307640; RRID:AB_2561913
PE Mouse Anti-Human Granzyme B	BD Biosciences	Cat# 561142; RRID:AB_10561690
FITC Mouse anti-Human Granzyme B	BD Biosciences	Cat# 560211; RRID:AB_1645488
FOXP3 Monoclonal Antibody (236A/E7), PE-Cyanine7, eBioscience™	Thermo Fisher Scientific	Cat# 25-4777-41; RRID:AB_2573449
PE-CF594 Mouse Anti-Human FoxP3	BD Biosciences	Cat# 562421; RRID:AB_11153143
Alexa Fluor® 488 anti-human FOXP3 Antibody	BioLegend	Cat# 320211; RRID:AB_430886
BD™ PE Mouse Anti-Human bcl-2	BD Biosciences	Cat# 340576; RRID:AB_400061
FITC Mouse Anti-Ki-67 Set	BD Biosciences	Cat# 556026; RRID:AB_396302
Alexa Fluor® 647 Mouse anti-Ki-67	BD Biosciences	Cat# 558615; RRID:AB_647130
Alexa Fluor® 700 Mouse anti-Ki-67	BD Biosciences	Cat# 561277; RRID:AB_10611571
Alexa Fluor® 647 Mouse Anti-Stat5 (pY694)	BD Biosciences	Cat# 612599; RRID:AB_399882
IL-17A Monoclonal Antibody (eBio64DEC17), APC, eBioscience™	Thermo Fisher Scientific	Cat# 17-7179-42; RRID:AB_1582221
BV650 Rat Anti-Human IL-2	BD Biosciences	Cat# 564166; RRID:AB_2738637
IFN gamma Monoclonal Antibody (4S.B3), PE-Cyanine7, eBioscience™	Thermo Fisher Scientific	Cat# 25-7319-82; RRID:AB_469682
APC Mouse Anti-Human HLA-A2	BD Pharmingen	Cat# 561341; RRID:AB_10646036

(*Continued on next page*)

Continued

REAGENT or RESOURCE	SOURCE	IDENTIFIER
Alexa Fluor(R) 700 anti-human TNF-alpha	BioLegend	Cat# 502927; RRID:AB_2561314
eBioscience™ 7-AAD Viability Staining Solution	Thermo Fisher Scientific	Cat# 00-6993-50
Biological samples		
Healthy human peripheral blood (Buffy coat)	Croix rouge de Belgique	https://www.redcrossblood.org/biomedical-services/specialty-services/cell-and-gene-therapy-solutions/buffy-coats.html
Chemicals, peptides, and recombinant proteins		
Recombinant Human IL-2	Peprotech	Cat# 200–02
Mafosfamide Sodium Salt	Santa Cruz Biotechnology	Cat# sc-211761
Dynabeads™ Human T-Activator CD3/CD28 for T Cell Expansion and Activation	Thermo Fisher Scientific	Cat# 11131D
Cyclophosphamide (Endoxan)	Baxter	Cat# 10019095601
Proleukin® (Aldesleukin)	Prometheus	Cat# 65483011607
Beetle Luciferin, Potassium Salt	Promega	Cat# E1605
Ficoll® Paque Plus	Sigma-Aldrich	Cat# GE17-1440-03
Collagenase A from *Clostridium histolyticum*	Sigma-Aldrich	Cat# 10103586001
DNase I from bovine pancreas	Sigma-Aldrich	Cat# 11284932001
HBSS	Lonza	Cat#10–508F
RPMI Medium 1640	Thermo Fisher Scientific	Cat#42401–018
Fetal Bovine Serum	Sigma-Aldrich	Cat#F9665-500ML
Human Serum	Sigma-Aldrich	Cat#H4522-100ML
Pen Strep	Thermo Fisher Scientific	Cat#15140122
L-Glutamine 200 mM	Thermo Fisher Scientific	Cat#25030081
eBioscience™ 10X RBC Lysis Buffer (Multi-species)	Thermo Fisher Scientific	Cat#00-4300-54
Critical commercial assays		
EasySep™ Human T Cell Isolation Kit	Stemcell Technologies	Cat# 17951
EasySep™ Human CD3 Positive Selection Kit II	Stemcell Technologies	Cat# 17851
CellTrace™ CFSE Cell Proliferation Kit, for flow cytometry	Thermo Fisher Scientific	Cat# C34554
Human HS Cytokine A Premixed Mag Luminex Performance Assay,Analyte: IL-2, TNF-alpha, IFN-gamma	Bio-Techne Ltd	Cat# FCSTM09-03
EasySep™ Human Pan-CD25 Positive Selection and Depletion Kit	Stemcell Technologies	Cat# 17861
PureLink™ Genomic DNA Mini Kit	Thermo Fisher Scientific	Cat# K182001
Chromium Single Cell 3' Reagent Kits v3	10x Genomics	Cat# PN-1000075
KAPA Library QuanitifiCation Kits	Roche	Cat# KK4824
eBioscience™ Foxp3 / Transcription Factor Staining Buffer Set	Thermo Fisher Scientific	Cat#00-5523-00
eBioscience™ Cell Stimulation Cocktail (plus protein transport inhibitors)	Thermo Fisher Scientific	Cat#00-4975-93
PerFix EXPOSE (Phospho-Epitopes Exposure kit)	Beckman Coulter	Cat#B26976

(*Continued on next page*)

Continued

REAGENT or RESOURCE	SOURCE	IDENTIFIER
Deposited data		
TCRVB deep sequencing on human T cells isolated from humanized mice engrafted with human PBMC and treated or not with Cyclophosphamide post-transplantation	This study	https://doi.org/10.5281/zenodo.7061490
Single cell RNA-seq datas on human T cells isolated from humanized mice engrafted with human PBMC and treated or not with Cyclophosphamide post-transplantation	This study	https://www.ebi.ac.uk/biostudies/studies/E-MTAB-12188
Experimental models: Cell lines		
THP-1 transduced with lentiviral vectors allowing luciferase expression	our lab	https://www.tandfonline.com/doi/suppl/10.1080/2162402X.2017.1314425?scroll=top
Experimental models: Organisms/strains		
Mouse: NOD.Cg-*Prkdc*^{scid} *Il2rg*^{tm1Wjl}/SzJ Common Name: **NSG** (	The Jackson Laboratory	Strain #:005557,RRID:IMSR_JAX:005557
Mouse: NOD.Cg-*Prkdc*^{scid} *Il2rg*^{tm1Wjl} Tg(HLA-A/H2-D/B2M)1Dvs/SzJ Common Name: **NSG-HLA-A2/HHD**	The Jackson Laboratory	Strain #:014570,RRID:IMSR_JAX:014570
Mouse: NOD.Cg-*Prkdc*^{scid} *Il2rg*^{tm1Wjl} Tg(IL15)1Sz/SzJ Common Name: **NSG-Tg(Hu-IL15)**	The Jackson Laboratory	Strain #:030890,RRID:IMSR_JAX:030890
Software and algorithms		
FlowJo	BD Life Sciences	https://www.flowjo.com/
GraphPad Prism 8	GraphPad Software	https://www.graphpad.com/
immunoSEQ® Analyzer	Adaptive Biotechnologies	https://www.immunoseq.com/analyzer/
QIAxcel Software	Qiagen	Cat#9021165
CellRanger (2.2.0)	10X Genomics	http://software.10xgenomics.com/single-cell/overview/welcome
scanpy package	Wolf, F Alexander et al.,2018[54]	https://pypi.org/project/scanpy/
Seurat	Satija, R, Farell J.A., et al., 2015[55]	https://cran.r-project.org/web/packages/Seurat/index.html
Harmonypy	Korsunsky, Ilya et al.,2019[56]	https://github.com/slowkow/harmonypy
UMAP: Uniform Manifold Approximation and Projection for Dimension Reduction	Becht, Etienne et al.,2018[57]	https://arxiv.org/abs/1802.03426#:~:text=UMAP%20(Uniform%20Manifold%20Approximation%20and,applies%20to%20real%20world%20data
Leiden clustering	Traag VA, Waltman L, van Eck NJ, 2019[58]	https://cran.r-project.org/web/packages/leiden/vignettes/run_leiden.html
GSEA tool (4.2.3)	Subramanian, Aravind et al., 2005[60]	https://www.gsea-msigdb.org/gsea/index.jsp
xPONENT 4.0 software	Luminex	
Aura Imaging Software	spectral instruments imaging	https://spectralinvivo.com/software/

RESOURCE AVAILABILITY

Lead contact

Further information and requests for resources and reagents should be directed to and will be fulfilled by the lead contact, Baron Frédéric (f.baron@uliege.be).

Materials availability

This study did not generate new unique reagents.

Data and code availability

- Single-cell RNA-seq data are available in the BioStudies database (https://www.ebi.ac.uk/biostudies/) under accession number E-MTAB-12188 (https://www.ebi.ac.uk/biostudies/studies/E-MTAB-12188). Nucleotide sequence data of TCRVB are available on Zenodo at https://doi.org/10.5281/zenodo.7061490. Accession numbers are listed in the key resources table.
- This paper does not report original code.
- Any additional information required to reanalyze the data reported in this paper is available from the lead contact upon request.

EXPERIMENTAL MODEL AND SUBJECT DETAILS

Mice

NSG, NSG-HLA-A2/HDD and NSG-Tg (Hu-IL15) mice were purchased from The Jackson Laboratory (Bar Harbor, Maine, ME, USA). Mice were housed in pathogen-free conditions in microisolator cages and fed standard rodent chow diet. Female and male mice aged between 8-14 weeks were used for experiments. Mice were euthanized with an injection of pentobarbital (Dolethal^{R,} Vetoquinol, Niel, Belgium) injection followed by cervical dislocation. All animal experiments used in this study were reviewed and approved by the Institutional Animal Care and Use Ethics Committee of the University of Liege, Belgium (file # 19–2114). The "Guide for the Care and Use of Laboratory Animals," prepared by the Institute of Laboratory Animal Resources, National Research Council, and published by the National Academy Press, was followed cautiously.

Primary cell culture

The study has been approved by the Comité d'Ethique Hospitalo-Facultaire Universitaire de Liège (project # 2020/17). Peripheral blood was obtained from buffy coats provided by the Belgian Red Cross. PBMC were isolated by Ficoll density gradient centrifugation and resuspended in PBS+3%FBS staining buffer. $CD3^+$ T cells were isolated with the EasySep™ Human-T Cell Isolation Kit. Cells were counted with a Sysmex XS-800i and seeded in 96-well U bottom plates. Cells were cultured and activated in the presence of anti-CD3/CD28 beads (Bead-Cell ratio 1:10, 1:2) (Thermo Fisher) in RPMI 1640 medium, supplemented with L-glutamine (2mM), penicillin (100 U/mL), streptomycin (10 mg/mL), 5% human AB serum and 20 ng/mL IL-2 for 48h before stimulation with mafosfamide (an analog of cyclophosphamide with an endogenous activity).

METHOD DETAILS

Induction of xGVHD and PTCy administration

NSG or NSG-HLA-A2/HHD mice, aged from eight to 14 weeks were injected intravenously (i.v.) with 2×10^7 human PBMC (hPBMC) obtained from buffy coat. NSG-Tg (Hu-IL15) mice were injected i.v. with 1×10^7 or 2×10^7 hPBMC. In most experiments, no conditioning was given with the exception of experiments looking at the impact of PTCy administration on day six (mice sacrificed on day six) for which mice received 2 Gy total body irradiation approximately 24 hours before injection of 2×10^7 hPBMC (irradiation was performed in these experiments to increase engraftment in order to have more cells to analyze for flow-cytometry and RNA-seq experiments). GVHD severity was evaluated by a scoring system that incorporates four clinical parameters including weight loss, posture (hunching), mobility and anemia, as previously reported.[49] Each parameter received a score of zero (minimum) to two (maximum). Mice were assessed for GVHD scores thrice weekly and monitored daily during the experiments. Mice reaching a GVHD score of 6/8 or having lost more than 20% of their initial weight were sacrificed. Final scores for dead animals reaching the ethical limit score (6/8) were kept in the data set for the remaining time points.

Cyclophosphamide (Endoxan, Baxter, Illinois, IL, USA), dissolved in NaCl 0.9%, was administered intraperitoneally (i.p.) at 100 mg/kg on day three. For the experiment of PTCy in combination with low dose recombinant human IL-2, NSG mice received from day two to day 15 Proleukine (Aldesleukin, Prometheus laboratories, California, CA, USA) at the dose of 25 000 IU/mice i.p. in addition or not to a

single injection of PTCy on day three. Finally, in order to study the impact of Treg on xGVHD prevention by PTCy, NSG mice were infused with CD25-depleted hPBMC. CD25 depletion of hPBMC was performed by immunomagnetic selection with the EasySep™ Human Pan-CD25 Positive Selection and Depletion Kit (Stemcell Technologies, Vancouver, Canada).

Flow cytometry

In most experiments, peripheral blood (PB) draws were systematically performed on days seven, 14, and 21 (as well as on day 28 in some experiments). In some experiments, mice were systematically sacrificed on day six or 21 and PB, spleen, and bone marrow (BM) as well as liver and lungs (for sacrifice on day 21) were harvested at the time of necropsy. PB was depleted of erythrocytes with the RBC lysis buffer (Thermo Fisher, Massachusetts, MA, USA) according to the manufacturer's instructions. Splenocytes were obtained by crushing the spleen, and BM cells by flushing femurs and tibiae. Lung- and liver-infiltrating cells were obtained after enzymatic and mechanic tissue digestion by mincing and incubating the organs for one hour in HBSS +50 μg/mL DNase 1 (Roche, Basel, Switzerland) + 1mg/mL collagenase A (Roche). Digestions were stopped by washing twice with PBS + EDTA 10mM, pH = 7.3, and mononuclear white blood cells were obtained by Ficoll (GE Healthcare, Upsala, Sweden) gradient centrifugation. Cells from all organs were washed twice with PBS+3% FBS and were counted with ABX diagnostics - Micros 60 (AxonLab, Baden, Switzerland) before processing with the antibody staining. The antibodies used consisted of anti-CD45-BV510 (H130, Becton Dickinson (BD), New Jersey, NJ, USA); anti-CD3-APC (SK7,BD); anti-CD4-eFluor450 (RPA-T4, Thermo Fisher); anti-CD4-BV786 (SK3, BD); anti-CD8-PECy7 (SK1, Biolegend); anti-CD8-APC-Cy7 (SK1, BD); anti-CD8-PE (HIT8a, BD); anti-CD16-FITC (3G8, BD); anti-CD45RA-PE-CF594 (HI100, BD); anti-CD45RA-BV785 (HI100, Biolegend); anti-CD27-BV650 (M-T271, BD); anti-CD62L-APC-eFluor780 (DREG56, Thermo Fisher),anti-CD62L-BB515 (SK11, BD); anti-CD14-Efluor450 (61D3, Thermo Fisher); anti-CD25-BUV395 (2a3, BD); anti-CD56-APC-R700 (NCAM16.2, BD); anti-HLA-DR-BV605 (L243, Biolegend, California, CA, USA); anti-GRANZYME B-PE (GB11, BD); anti-GRANZYME B-FITC (GB11,BD); anti-FOXP3-AlexaFluor488 (206D, Biolegend); anti-FOXP3-PE-Cy7 (236A/E7, Thermo Fisher); anti-FOXP3-PE-CF594 (259D/C7, BD); anti-BCL-2-PE (100, BD); anti-Ki67-FITC (B56, BD); anti-Ki67-AlexaFluor647 (B56, BD); anti-Ki67-AlexaFluor700 (B56, BD); anti-phosphoSTAT5-Alexafluor647 (47/Stat5(pY694), BD) anti-IL-17-APC (eBio64DEC17, Thermo Fisher); anti-IL-2-BV650 (5344.111, BD); anti-IFNg-PECy7 (4S.B3, Thermo Fisher); anti-TNF-AF700 (MAb11, Biolegend). The following antibody specific for mouse antigens was used: anti-CD45-PECy5 (30-F11, BD). Mixes of extracellular antibodies were done in brilliant stain buffer (BD, 50 μL/sample). Cells were incubated with surface antibodies for 20 min at 4°C in the dark and washed twice with PBS+3% FBS. Intracellular and cytokines staining was performed by using the FOXP3 Staining Buffer Set according to the manufacturer's instructions (Thermo Fisher). For intracellular cytokine staining, cells were stimulated for 4h in RPMI supplemented with 10% FBS, penicillin (100 U/mL), streptomycin (10 mg/mL) and in the presence of PMA/ionomycin, brefeldin A, and monensin (Cell Stimulation Cocktail + Protein Transport Inhibitors, Thermo Fisher).

For pSTAT5 staining, the PerFix EXPOSE reagent kit (PFE, Beckman Coulter, CA, USA) was used according to the manufacturer's instructions.

Total cell counts of human $CD45^+$ cells in PB were calculated based on the absolute number of white blood cells (counted by using ABX diagnostics - Micros 60) and on human cell chimerism (frequency of human $CD45^+/(\%_{human}CD45^+ + \%_{mouse}CD45^+)$). Data were acquired on FACS LSRFortessa (BD) and were analyzed with FlowJo v10.6.1 (BD). In gating strategies, Tregs were defined as $CD4^+CD25^+FOXP3^+$ cells while the remaining $CD4^+$ T cells were termed conventional T cells (Tconv). Naive T cells (T_{naive}) were defined as $CD45RA^+CD27^+$, effector T cells (TEFF) as $CD45RA^-CD27^-$, effector memory T cells (TEM) as $CD45RA^-CD27^+CD62L^-$, and central memory T cells (TCM) as $CD45RA^-CD27^+CD62L^+$ T cells.

Serum cytokine levels

The concentration of human cytokines (IL-2, TNF-alpha, IFN-gamma) was determined in mouse serum on days 6 and 28, after a 2-fold dilution, using a custom Magnetic Luminex Performance Assay (R&D Systems, Minneapolis, MN, USA). The experiments were performed according to the manufacturer's recommendations, and results were acquired on the Luminex MAGPIX system and analyzed with the Luminex xPonent Software 4.0.

CFSE proliferation assay

T cells were labeled with CFSE 5 μM (Thermo Fisher) just after their isolation and seeded in culture as mentioned above with CD3/CD28 beads (bead-cell ratio 1:10, 1:2). After 48h hours in culture, cells were treated or not with mafosfamide (Santa Cruz Biotechnology, Texas, TX, USA) at 4 or 8 μg/mL overnight. Finally, cells were harvested and stained with 7-AAD and analyzed by flow cytometry on a CytoFLEX (Beckman Coulter) to measure the number of live cells/well. In addition, cells were stained with CD4, CD8, CD25, KI67, FOXP3 to separate Tconv ($CD4^+FOXP3^-$) from Treg cells ($CD4^+CD25^+FOXP3^+$) and to analyze CFSE signaling in each cell population by flow cytometry. The inhibition of proliferation induced by mafosfamide was calculated with the following formula: 100 x (1 − %$CFSE^{high}$ cells treated / %$CFSE^{high}$ cells untreated).

TCR repertoire diversity

Spleens and lungs from 10 NSG mice per group (control or treated with 100 mg/kg PTCy) were collected at day 21, pooled together, and were stained with anti-CD45, -CD3, -CD4, and -CD8 antibodies for flow cytometry sorting on a FACS ARIA II (BD). A total of 3 × 10^6 $CD45^+CD3^+CD4^+$ and $CD45^+CD3^+CD8^+$ T cells were sorted from each organ. The same cell populations were also sorted before transplantation from the PBMC of the donor. DNA was extracted using the PureLink Genomic DNA Mini Kit (Thermo Fisher). One hundred fifty μg from each sample were used for T-cell receptor Vβ (TCRVB) deep sequencing performed by Adaptive Biotechnologies (Seattle, Washington, WA, USA).

For data analysis, the productive clonality output of the ImmunoSeq analyzer of Adaptive Biotech was used as is. This clonality is computed by using Simpson's diversity index on the rearrangements able to encode a functional protein (productive). This includes only in-frame rearrangements and excludes those containing a stop codon or a frameshift mutation. The Simpson diversity index[50] is calculated by weighted arithmetic mean of each squared clone abundance, yielding values between zero and one (zero indicates greater diversity and one indicates lower diversity of the repertoire).

The differential expansion analyses used to identify xenoreactive clonotypes were made with the "Differential abundance" tool of the ImmunoSeq analyzer of Adaptive Biotech, with default parameters (two-sided binomial method, productive clonotypes only, nucleotide counts, minTotal = 10, benjamini-hochberg correction of p-values, significance set at 0.01). This tool compares two samples and identifies rearrangements (unique sequences) that have significantly increased or decreased in frequency. This comparison is performed through the usage of exact Fisher tests on the abundance values of each clonotypes, against the null hypothesis that the population abundance of the clone is identical in the two samples compared. This method has been described in details in the section "identification of expanded and enriched effector T-cell clones" of reference.[51] p-values of Fisher tests were corrected for multiple testing with the False Discovery Rate (FDR) method of Benjamini & Hochberg.[52] Xenoreactive clonotypes were defined as clonotypes significantly (FDR<0.01) expanded in control mice organs vs donor PBMCs while bystanders were defined as clonotypes significantly contracted in mouse organs vs donor PBMCs.

Single cell RNA-Seq

Library preparation

Human $CD3^+$ T cells were isolated by immunomagnetic selection on day +6 from spleen of mice injected with 2 × 10^7 hPBMC and treated or not with PTCy on day +3. Isolated cells were washed once with PBS +0.04% BSA. Cell concentration was adjusted to 1,000 total cells/μL and 13,300 cells were loaded on Chromium Controller (10X Genomics). Amplified cDNA quality controls were performed with an Agilent bioanalyzer and final library profiled were checked on Qiaxcel (Qiagen). Sequencing libraries were loaded in Illumina Novaseq sequencer with NovaSeq SP 100 v1 kit (Illumina, CA, USA) using the following read lengths: 28 bp for Read1 (16 bp Barcode +12 bp Randomer), 8 bp for Sample Index and 80 bp for Read2. Library quantification was processed with KAPA Library quantification kit (KAPA Biosystems).

Data pre-processing

Demultiplexing, alignment to a reference genome, and gene quantification steps were taken using CellRanger (2.2.0)[53] with a custom reference package based on the human reference genome GRCh38. Further data processing steps were conducted using *Scanpy* (1.8.2) library.[54] Viable cells were separated from the empty droplets by filtering based on genes number >350, counts number >500, and

mitochondrial proportion <20%. The raw counts were normalized using CPM normalization with the scale factor of 10^4 and transformed to log scale using log1p function from Scanpy library. Highly variable genes were selected with the flavor "Seurat"[55] and used for principal component analysis (PCA), for dimensionality reduction.

Identification of cell cycle states and cell types

For the identification of the cell types, batch correction is applied using the python version of Harmony (Harmonypy)[56] with default parameters. A neighborhood graph was generated using n_neighbours = 15 with cosine distance metric. The data were projected onto two-dimensional space using Uniform Approximation and Projection (UMAP) method.[57] Cells were grouped by Leiden clustering[58] and the highly expressed genes for each cluster were determined using rank_genes_groups function from Scanpy library with normalized data. To categorize the cells based on cell cycle states, Scanpy's *score_genes_cell_cycle* function was performed with the marker genes defined by Tirosh et al.[59]

Gene set scoring and enrichment analyses

scanpy's score gene function was used to assign an overall expression score for each hallmark gene set. Gene set enrichment analysis (GSEA) was performed by using the GSEA (4.2.3) tool.[60]

GvL effects and bioluminescence imaging

For GvL effect assessment, NSG-HLA-A2/HHD mice were co-injected with 3×10^6 luciferase-expressing THP-1 cells with or without 2×10^7 hPBMC from non-HLA-A02 donor on day 0. The hPBMC donors were selected by staining the hPBMC with anti-HLA-A2 APC (BB7.2, BD) antibodies. Mice were treated or not on day +3 with an i.p. injection of PTCy (100 mg/kg) and received a second injection of 2×10^6 THP-1 expressing luciferase on day +5. Survival and bioluminescence analyses were made as previously reported.[33] In brief, mice were injected subcutaneously with 3 mg of D-luciferin (Promega, WI, USA) in PBS and imaged 12 minutes later. Tumor growth was evaluated by measuring bioluminescence of THP-1 cell line transfected to express the luciferase reporter gene by using the bioluminescent IVIS imaging system (Xenogen-Caliper, Massachusetts, MA, USA). Mice were anesthetized using isoflurane (2.5% vaporized in O2) during bioluminescence analyses. For analysis, total photon flux (photons per second) was measured from the whole animal using Aura imaging software.

QUANTIFICATION AND STATISTICAL ANALYSIS

The Mann-Whitney test was used to compare flow-cytometry data and serum cytokine levels between two groups. Comparisons between GVHD score curves were made using the 2-way ANOVA test. Survival curves were modeled using the Kaplan-Meier method. Comparisons between groups were made with the log-rank test. Comparisons between cells in cultures were made with the 2-way ANOVA test and multiple comparisons with Sidak's or Tukey's multiple comparisons test. The Kruskal-Wallis test was used for Bioluminescence data. p values <0.05 were considered statistically significant and all p values were 2-sided. Statistical analyses were carried out with Graphpad Prism 8.3 (Graphpad Software, San Diego, CA, USA).